APPLICATION OF BIOCHAR FOR THE REMOVAL OF TOXIC POLLUTANTS FROM WATER

Charitha Tharanga Karunarathna Pathirannahalage

MSc Thesis

Biology of Environmental Change

University of Eastern Finland, Faculty of Science and Forestry

Department of Environmental and Biological Sciences

August 2020

UNIVERSITY OF EASTERN FINLAND, Faculty of Science and Forestry
Master's Degree Programme in Biology of Environmental Change
Charitha Pathirannahalage: Application of biochar for the removal of toxic pollutants from water
MSc thesis: 57 pages
Supervisors: Professor Amit Bhatnagar, PhD
Dr Ali Maged
August 2020

Keywords: Biochar; Adsorption, Water treatment, Lead, Crystal violet.

ABSTRACT

Increased use of lead (Pb(II)) in industrial applications has resulted high concentrations of Pb(II) in water. High consumption of Crystal violet dye in the textile and dyeing industries has also caused serious water pollution. Hence, removal of these two pollutants from water is important. Adsorption potential of Pb(II) and Crystal violet from water using biochar, generated from paper mill sludge from Korea (PSK), as an adsorbent was studied in this study. Batch studies have been performed to describe the impact of different parameters such as the effect of solution pH, adsorbent dosage, initial concentration, contact time and ionic strength on the removal of Pb(II) and Crystal violet. The optimized pH was 5.5 and 7.0 for Pb(II) and Crystal violet, respectively. Adsorbent dose was selected as 0.1 g/L for all three PSK biochars. The adsorption data was well fitted to the Langmuir isotherm model. The maximum adsorption capacities were 454.55 mg/g and 1000 mg/g for Pb(II) and Crystal violet, respectively. Kinetic studies showed that the interaction of Pb(II) and Crystal violet with all three PSK biochars obeyed pseudo second-order kinetic model. Further, the adsorption process of Pb(II) and Crystal violet do not obey the intraparticle diffusion model. Presence of co-existing ions affected the efficiency of all three PSK biochars on the removal of Pb(II) and Crystal violet from water, which led to a considerable decrease in adsorption capacity.

ACKNOWLEDGMENTS

I would like to express my heartiest gratitude to my research supervisor Prof. Amit Bhatnagar, Department of Environmental and Biological Sciences, Faculty of Science and Forestry, University of Eastern Finland. Without his enthusiasm, inspiration, and great effort to explain things clearly and simply it would have been impossible for me to finish this work. I am also grateful to Dr. Ali Maged, throughout my research work he provided me encouragement, sound advice, good teaching, good companionship, and lots of good ideas. This total outcome would not be possible without their motivation and excellent guidance.

My sincere gratitude goes to Prof. Yong Sik Ok, Korea University, South Korea, for providing the biochar samples. I would like to extend my thanks to all academic and non-academic staff members of the Department of Environmental and Biological Sciences for their assistance given during this research period.

It is a failure of me if I do not extend my gratefulness to my colleagues of the water chemistry research group. Finally, I would like to extend my deepest appreciation to my loving parents, wife, family members and friends for their great moral support, love, patient, and encouragement to persuade my interest in this research.

LIST OF ABBREVIATIONS

g	gram
kg	kilograms
LD_{50}	Lethal Dose
M	Molar concentration
mg/L	milligrams per liter
nm	nanometer
PSK	Paper mill Sludge Korea
°C	degree Celsius

CONTENT

1 INTRODUCTION

The global population has been accelerating at an alarming rate and it is estimated that the world population will be around 8.9 billion by 2050 (Postel, 2000). As a result, natural resources such as air, water, coal, forests, etc. are depleting extensively due to the higher consumption rate and anthropogenic activities. Among them, water plays a vital role in our life. Even though water resources are available all over the world, most water is found in seas. However, sea water is not suitable for drinking purposes and freshwater resources are limited and polluted. Therefore the sustainable ways should be used to provide a new source of clean water. The inferior water management practices have caused freshwater pollution, creating a critical issue globally, especially in the developing countries.

Water pollution is a key area of concern aligned with the industrial development of any country. Metal processing, paper, mining operations, batteries, textile, leather, industries, etc., generate a huge volume of wastewaters, which release a vast amount of chemicals in the natural water bodies, causing a significant impact on the aquatic environment. Among many pollutants, heavy metals and dyes have gained much interest in the water pollution entailed with industrial development. Due to persistence in nature, they cause adverse impacts on humans', animals', and plants' health.

Coagulation, chemical precipitation, ion exchange, reverse osmosis, flocculation, etc., are currently being used for removing dyes and heavy metals from water. However, these methods are expensive and could produce toxic sludge in the treatment process. As a result, attention has been focused on alternative methods such as adsorption by biochar, derived from biowaste materials, food waste, paper mill sludge, agriculture waste etc. Adsorption using biochar is considered as one of the best processes to eliminate dyes and heavy metals from contaminated water due to low operational cost, environmentally friendly and simple process.

Lead is a useful heavy metal which occurs naturally and may cause severe health risks. Even though the amount of lead in natural water is low, industrial waste and applications of lead-based products have resulted an increase concentration of Pb(II) in water. Crystal violet is one of the commonly utilized dyes in the textile, and dyeing industries and has been identified as a highly toxic dye. Hence, the removal of Pb(II) and Crystal violet from water is important.

2 LITERATURE REVIEW

2.1 Water pollution

Among many environmental issues, water quality and quantity are the prominent issues faced by people in the twenty-first century. Agriculture, industrial and domestic activities are using more than one-third of the earth's reachable fresh water. As a result, these actions have caused water pollution with various artificial and geogenic natural chemicals. It is estimated that safe drinking water is not available for more than one third of the population in the world (Schwarzenbach *et al.*, 2010). Due to the high expansion of industries: pesticides, mining, fertilizer, batteries, etc., heavy metals are either indirectly or directly discharged to natural water bodies. Different heavy metals e.g. zinc, nickel, copper, lead, mercury, chromium, and cadmium are commonly observed in wastewater streams (Fu and Wang, 2011).

In addition to the inorganic contaminants, organic pollutants, such as synthetic dyes have created lots of adverse effects on the water environment (Alshabanat *et al*., 2013). Huge amounts (up to 50000 tons) of synthetic dyes are regularly discharged to water streams due to inappropriate management of textile, food, paper, and pharmaceutical industries. These dyes are hard to decolorize because of aromatic rings and complex structures, causing mutagenic and carcinogenic effects (Mittal *et al.*, 2010). Moreover, dyes have affected the aquatic ecosystems, due to disturbing the light penetration into the water (Mittal *et al.*, 2010; Wathukarage *et al.*, 2019).

2.2 General properties of heavy metals

Heavy metals are naturally occurring elements that can be found all around the earth's crust. These are classified as metallic elements that have a higher density than water. Even though heavy metals include metallic elements, arsenic like metalloids also fall under this category (Tchounwou *et al*., 2012). Heavy metals have an atomic weight between 63.5 and 200.6 and a specific gravity of more than 5. Most heavy metals are either hazardous or carcinogenic due to non-biodegradability and bioaccumulation in living organisms (Fu and Wang, 2011). Although heavy metals occur in a natural environment for years undisturbed, exponential development in agriculture, technological, mining, industrial, and household applications is the reason for exposure (Tchounwou *et al*., 2012).

Heavy metals are regarded as trace elements when existing in little concentrations in a variety of environmental forms such as soil, water, plants etc. The concentrations in 'ppb' range to a lesser amount of 10 ppm levels are mostly present in the environment. In literature, it has been reported that metals, such as cobalt (Co), copper (Cu), chromium (Cr), iron (Fe), magnesium (Mg), manganese (Mn), molybdenum (Mo), nickel (Ni), selenium (Se) and zinc (Zn) are essential micro-nutrients for various biochemical and physiological functions (Tchounwou *et al*., 2012). An insufficient supply of these micro-nutrients could result in a variety of deficiency diseases or syndromes. Also, the indispensable heavy metals influenced biochemical and physiological functions in animals and plants, such a way that they are significant elements of some major enzymes and perform vital tasks in diverse oxidation-reduction reactions in living beings. However, when present in excess level, heavy metals may cause adverse impacts on animals' and humans' health (Tchounwou *et al*., 2012).

Along with the accelerated use, considerable quantities of heavy metals can be found in wastewaters which contain lead, cadmium, arsenic, copper, chromium, nickel, and zinc, causing hazardous impacts on the health of humans as well environment (Jaishankar *et al*., 2014). As a result, these elements are categorized as the most influential pollutants which are used to describe the quality of water, air, and soil (Sekar *et al*., 2014).

2.3 Adverse impacts of heavy metals

Heavy metal pollution is a rapidly growing problem, especially in aquatic environments due to the discharge activities from industries, domestic and agriculture which easily end up in the natural water resources. Ultimately, it causes direct water pollution in the first instance and subsequently transfers to the sediment phase, subject to possible accumulation over time. These heavy metal-based pollutants include Pb, Ni, Cd, Cu, Cr, As and Zn which pose the highest risk among the chemical exhaustive industries (Barakat, 2011).

Heavy metals are different from organic wastes due to their non-biodegradability and high solubility in the aqueous phase, thereby these are always found in the aquatic environment. In addition, heavy metals can be deposited in the food chain, causing disorders and diseases in animals and humans (Ngah and Hanafiah, 2008). Main health problems from heavy metals' toxicity are injury or decline mental and central nervous functions, cancers, lower energy levels etc. Also, harming to the blood composition, kidney, lungs, liver, and other essential organs (Amarasinghe and Williams, 2007). The most common instance is damaging to the gills of

aquatic fauna like fish. Therefore, it is crucial to purify wastewater contaminated with heavy metals prior to discharge (Amarasinghe and Williams, 2007; Barakat, 2011; Ngah and Hanafiah, 2008). Among heavy metals, lead has been recognized as toxic metal, which can cause damage in the brain functions, liver, reproductive system, central nervous system, failure of kidney and basic cellular processes (Fu and Wang, 2011).

2.4 General properties of lead

Lead comprises four stable isotopes namely, ^{204} Pb, ^{206} Pb, ^{207} Pb and ^{208} Pb. This mixture varies according to the geological regions (Renberg *et al.*, 2002). Lead, frequently found in water, soil and plants at trace levels, is a natural component of the crust of the earth. The main lead ore minerals are cerussite ($PbCO_3$) and galena (PbS). Lead can be found in ores which contain zinc, copper and silver. Therefore, lead can be extracted as a core product of these metals (Cheng and Hu, 2010).

Lead is greatly ductile, malleable, and simple to smelt (Cheng and Hu, 2010). Lead can be observed as bright silver color in a dry atmosphere. Lead is considered as a highly toxic metal that has a health impact in many parts of the world. Major sources of lead are battery industries, metal plating and finishing, fertilizer, pesticide industries, smelting of ores, factory chimneys, gasoline, and automobiles (Jaishankar *et al.*, 2014). In addition, lead is originated from anthropogenic activities such as waste incineration and coal burning (Cheng and Hu, 2010). When releasing lead into the environment, it is taken up by plants, soil, and water. As a result, humans are exposed to lead via either food or water (Jaishankar *et al.*, 2014).

2.5 Application of lead

Lead is one of the seven metals of antiquity which was used before copper and bronze. The earliest lead artifact was reported in 6500 B.C, while the processing of lead minerals was started 6000 years ago (Cheng and Hu, 2010). According to the international lead and zinc study group in 2010, about 8.757 million tons of lead have been used and consumed all over the world (Gupta *et al*., 2011).

Use of lead-containing water pipes has been banded. However, lead has been used in other applications extensively. In the industrial sector, lead has been used for printing, dyeing, painting, ceramic and glass industries, ammunition, tetraethyl lead manufacturing, acid metal plating, and finishing (Gupta *et al*., 2011). In addition, lead is commonly used to manufacture

lead-acid batteries, building constructions, solder bullets and shot, weights, fusible alloys, and pewter (Cheng and Hu, 2010).

2.6 Effect of lead on the environment

In literature, it is reported that lead has become the most scattered hazardous metal in the world due to anthropogenic activities (Cheng and Hu, 2010). Poisoning of lead can be found dating back to the Roman era (Gidlow, 2004). The poisonous symptoms from lead are dizziness, insomnia, headache, and anemia (Fu and Wang, 2011). Toxic metals like lead and mercury can cause autoimmunity, in which immune system strikes its own cells, leading to joint diseases such as rheumatoid arthritis (Barakat, 2011).

Unlike other metals such as copper, zinc and manganese, lead is extremely toxic to the plants. High concentration levels of lead in plants can damage the chlorophyll, photosynthesis process and suppress the growth of the plants ultimately. It reveals that even at a low concentration, lead can cause instable of ion uptake by plants (Jaishankar *et al.*, 2014).

2.7 General properties of dyes

Dyes can be categorized corresponding to their chemical structure and application or their usage. However, chemical structure is considered as the most suitable method for the classification of dyes (Gregory, 1990; Hunger, 2000). In the chemical classification, synthetic dyes, which have stable and different chemical structures, have been categorized by their chromophores (Wong and Yu, 1999). In the classification of application methods, dyes are grouped as non-ionic (disperse dyes), cationic (basic dyes) and anionic (direct, acid, and reactive dyes) (Mall *et al*., 2006). Chemical classes of dyes in the industrial scale are triphenylmethyl, anthraquinone, azo, sulfur, indigoid and phthalocyanine derivative (Gregory,1990).

Synthetic dyes are highly stable in the environment due to their complex aromatic compounds (Wathukarage *et al.*, 2019). Concentration level 10 - 50 mg/L of dye is greatly visible in water. Due to containing nitro and sulfonic groups in dyes, they cannot be uniformly decomposed in the conventional aerobic process (Wong and Yu, 1999).

Textile, plastics, leather, paint, acrylic, cosmetics, pharmaceutical, paper, industries commonly use dyes for coloring their products accompanied by a considerable volume of water.

As a result, it is evaluated that approximately 30% of world dye production is wasted during the processing stages, persisting 10 - 50 mg/L dye concentration in effluents (Wathukarage *et al.*, 2019). Among the diverse industries, dyes are mainly generated from the printing and textile industries (Cheung *et al*., 2007). It is estimated that consumption of the dye is about 10,000,000 kg/year from the textile industry, and about 1,000,000 kg/year of dyes are released into waste flows (Hameed *et al*., 2007). In addition, synthetic dyes are used for the discovery of the particular surface area of activated sludge for groundwater tracking (Forgacs *et al*., 2004).

2.8 Adverse impacts of dyes

Industrial wastewater commonly comprises different type of hazardous chemicals and organic compounds which are toxic to aquatic species and fish population (Hameed *et al*., 2007). The artificial dye is considered as one of the most significant pollutants in the aquatic environment owing to massive production, ample applications, business value, less biodegradable nature and toxicity. Therefore, these dyes consist of triphenylmethane, heterocyclic, azo, anthraquinone and polymeric that can contaminate groundwater, soil and drinking water supplies (Tan *et al.*, 2016). Contamination of water caused by synthetic dyes has become a critical issue since it causes an adverse effect on public health as well as harm to the environment (Chakraborty *et al*., 2011). The dyes can be mutagenic, teratogenic, carcinogenic, which causes allergic reactions on living organisms (Wathukarage *et al.*, 2019). In addition, dyes can bioaccumulate in wildlife and can cause negative eco-toxicological effects (Chakraborty *et al*., 2011).

Color is the most visible parameter of water pollution. Discharging color waste to water bodies can reduce the aesthetic value. Dyes can affect the transmission of lights into the water bodies, reducing photosynthesis activities and disturbing aquatic life (Mall *et al*., 2006). Moreover, dyes can decrease the solubility of water bodies (Wong and Yu, 1999) and dyes are one of the sources of eutrophication (Chakraborty *et al*., 2011). Among several dyes, Crystal violet has been recognized as a toxic dye, which is liable for occurring slight eye inflammation, excruciating sensitization to the light (Mittal *et al.*, 2010).

2.9 General Properties of Crystal violet

Crystal violet belongs to the triphenylmethane class (Mittal *et al.*, 2010). It is well recognized as gentian violet, aniline violet, methyl violet or hexamethylpararosaniline chloride (Tan *et al.*, 2016).

Table 2.1: General properties of Crystal violet

IUPCA name	Molecular formula	Molecular weight
N-[4-[bis[4-dimethyl-amino)-phenyl]-methylene]-2,5-cyclohexadien-1-ylidine]-N methyl methanaminium chloride	$C_{25}H_{30}N_3Cl$	407.98 g/mol

Source : Mittal *et al.*, 2010

Crystal violet is a non-biodegradable dye which is categorized as a recalcitrant molece due to poor metabolization performed by microbes (Chakraborty *et al*., 2011). Crystal violet is a water-soluble and cationic dye (Wathukarage *et al.*, 2019; Vyavahare *et al.*, 2019). Cationic dyes are highly toxic than anionic dyes, showing high tinctorial values (< 1 mg/L). Crystal violet shows high-level color intensity, and it is extremely visible in aqueous solutions even in low concentrations, causing serious color pollution (Wathukarage *et al.*, 2019). The maximum absorption range of Crystal violet is between 589 and 594 nm (Mittal *et al.*, 2010).

2.10 Application of Crystal violet

Crystal violet is one of the commonly utilized dyes in the painting, textile, dying industries and biological staining (Wathukarage *et al.*, 2019; Vyavahare *et al.*, 2019). Crystal violet is employed as a purple color dye especially in the textile industry dyeing for cotton and silk (Chakraborty *et al*., 2011; Mittal *et al.*, 2010). Also, it is utilized as manufacturing inks and paints (Chakraborty *et al*., 2011). Furthermore, Crystal violet can be used as a pH indicator (Mittal *et al.*, 2010; Tan *et al.*, 2016; Vyavahare *et al.*, 2019).

In the medical sector, Crystal violet is applied as biological stain and an effective component in gram's stain. In veterinary and animal medicine, it acts as a bacteriostatic agent (Chakraborty *et al*., 2011). In addition, Crystal violet can be applied as an exterior skin sterilizer in animals and humans (Mittal *et al.*, 2010). Moreover, it can be manipulated as an additive to poultry feed to hinder the transmission of fungus, mold, and stomach parasites. Due to the protein-dye, Crystal violet can be utilized as a booster for bloody fingerprints (Chakraborty *et al*., 2011).

2.11 Effect of Crystal violet on the environment

The toxicity of Crystal violet can be attributed to the oxidative stress created by reactive oxygen species (Vyavahare *et al.*, 2019). Cornea and conjunctiva can be permanently damaged since Crystal violet is a cationic dye which has been identified as highly toxic to mammalian cells (Mittal *et al.*, 2010). According to literature, the poisonousness of single oral doses of Crystal violet for mice (LD_{50}) and rats (LD_{50}) has been reported as 1.2 g and 1.0 g per kg, respectively (Tan *et al.*, 2016). In addition, permanent blindness, kidney, and respiratory failure are identified as extreme cases (Mittal *et al.*, 2010). Inhaling of Crystal violet shows carcinogenic effects, irritation of respiratory and gastrointestinal tract and pain (Vyavahare *et al.*, 2019). Moreover, Crystal violet can enter via the skin, causing skin irritation and digestive tract irritation (Mittal *et al.*, 2010).

Due to the non-biodegradability, Crystal violet can persist in diverse environments for a long time (Chakraborty *et al*., 2011). Finally, it may enter the food chain leading to biomagnification and bioaccumulation in humans and wildlife. In aquatic ecosystems, primary production on fauna and flora is declined due to less penetration of sunlight into water columns (Wathukarage *et al.*, 2019). It has been reported that Crystal violet has caused groundwater contamination due to dye manufacturing activities in Basel (Tan *et al.*, 2016).

2.12 Treatment methods for dyes and heavy metals removal

Many approaches were used for the elimination of dyes from wastewater including biological, physicochemical, and chemical methods, i.e. activated sludge, photo-degradation, trickling filter, carbon adsorption and chemical coagulation, electrochemical techniques, flocculation, ozonation, precipitation, membrane filtration, and fungal decolorization, solar photo-Fenton, cation exchange membranes, solvent extraction, photocatalytic degradation, micellar enhanced ultra-filtration, reverse osmosis, sonochemical degradation and integrated iron(III) photo assisted-biological treatment (Chakraborty *et al*., 2011; Cheung *et al*., 2007; Hameed *et al*., 2007).

Photo-degradation, oxidative degradation, biochemical degradation, and electrocoagulation methods are not feasible to remove dyes from water due to high energy and chemical consumption on larger scales (Mittal *et al.*, 2010). Owing to the existence of heat and light stable, synthetic dyes are resistant to biodegradation. Thus, conventional treatments in sewerage plants such as primary and secondary treatments cannot be used to remove dye from water

(Cheung *et al*., 2007; Mall *et al*., 2006). Adsorption using activated carbon is an efficient practice to eradicate the dye from wastewater. However, activated carbon is a high-cost adsorbent (Cheung *et al*., 2007). Therefore, simple design, low-cost operation and environmentally friendly treatment methods using cheaper adsorbents are needed for the removal of dyes from wastewater (Mittal *et al.*, 2010).

A variety of methods are available for the elimination of heavy metals from wastewater. The commonly utilized methods are biosorption, ion exchange, chemical precipitation, flotation, solvent extraction, flocculation, reverse osmosis, coagulation, membrane separation, adsorption using activated carbon, cementation onto iron and electrolytic methods (Bello and Ojedoku, 2015). Among these methods, reverse osmosis and chemical precipitation are inefficient methods with the low concentrations of pollutants (Wasewar, 2010). By considering the efficiency and cost-effectiveness, researchers are interested in the development of new methods to substitute costly wastewater treatment procedures such as reverse osmosis, solvent extraction, membrane separation, ion exchange, chemical precipitation, electro flotation and electrodialysis (Kalavathy *et al*., 2005; Malkoc and Nuhoglu, 2005; Ngah and Hanafiah, 2008).

2.13 Adsorption

Adsorption is considered as one of the physical treatment processes (Ngah and Hanafiah, 2008). Among the high-cost removal methods, the adsorption is selected as a comparatively best alternative to decontaminate heavy metals and dyes from wastewater due to convenience, simple design, sludge freeness and low cost (Chakraborty *et al*., 2011; Hameed and Foo, 2010; Varma *et al*., 2013; Wasewar, 2010).

Adsorption is the process of accumulating substance from an ambient fluid phase on an appropriate surface of a solid (Parmar and Thakur, 2013). Adsorption can be more described as a procedure that occurs when a gas or liquid solute, which is called adsorbate, accumulates on the surface of an adsorbent (solid or a liquid) developing an atomic or molecular film. This process is distinct from absorption, in which an element diffuses into a solid or liquid. These two processes are linked together to describe the term sorption. Then the opposite process of sorption is described as desorption (Thommes *et al*., 2015).

Adsorption is functioning in most natural, biological, chemical, and physical systems (Elmoris *et al*., 2014). When the adsorption process occurs at a biological product, it is referred to biosorption, the adsorbent becomes biosorbent. Biosorbents are extremely porous materials

and adsorption fundamentally occurs either on the walls of the pores or at certain sites inside the particles (Jaman *et al*., 2009). Depending on the strength of the interactions between adsorbent and adsorbate, two types of adsorption are described, i.e. physical adsorption and chemical adsorption (Thommes *et al*., 2015).

2.13.1 Physical adsorption (Physisorption)

Physical adsorption is relatively non-specific. This occurs via intermolecular forces of attraction among molecules of the adsorbate and the adsorbent. These molecular attractive forces on the surface of adsorbent are merely physical in nature and van der Waals forces. This process does not require activation energy and the phenomenon is reversible (Králik, 2014).

2.13.2 Chemical adsorption (Chemisorption)

Chemical adsorption is the formation of chemical bonds because of intermolecular forces between the solid and adsorbed substances (Thommes *et al*., 2015). This type of adsorption is mostly important in catalysis. Chemisorption is an irreversible process and the elementary step is often involving large activation energy (Králik, 2014).

2.14 Adsorption by means of low-cost materials

The utilization of natural materials for the removal of heavy metals, dyes and other contaminants is becoming important in all countries. Although elatively expensive adsorbents show higher adsorption capacities, some natural materials or certain waste materials available in great quantities, can be applied as low-cost adsorbents. They represent widely available unexploited resources and are environmentally friendly (Elmorsi *et al*., 2014).

Adsorption is a low-cost process when it uses comparatively costless materials. The preparation of adsorbent material is generally effortless and does not require any more resources, chemicals, or processes (Zou *et al*., 2006). Instead of the widely used industrial sorbent e.g., activated carbon, many researchers have investigated numerous low-cost adsorbents, i.e. rice straw (Ahluwalia and Goya, 2005; Mittal *et al.*, 2010), paper mill sludge, sugarcane bagasse, peanut hulls (Ahluwalia and Goya, 2005; Chakraborty *et al*., 2011), sawdust (Malkoc and Nuhoglu, 2005; Mittal *et al.*, 2010), sugar industry waste (Chakraborty *et al*., 2011; Malkoc and Nuhoglu, 2005), coconut husk (Alshabanat *et al*., 2013; Thakur and Semil, 2013; Wathukarage *et al.*, 2019), agriculture-based waste materials (Chakraborty *et al*., 2011; Demirbas, 2008) and tea

factory waste (Chakraborty *et al*., 2011; Nandal *et al*., 2014; Sewu *et al.*, 2017) in order to remove heavy metals and dyes from wastewater.

2.15 The utilized adsorbents for removal of Crystal violet and lead

In literature, it has been reported that various type of adsorbent materials have been used to remove Crystal violet from wastewater. For examples, de-oiled soya and bottom ash (Mittal *et al.*, 2010), rice husk (Chakraborty *et al*., 2011), date palm fiber (Alshabanat *et al*., 2013), mango leaves (Vyavahare *et al.*, 2019), woody tree (*Gliricidia sepium*), grapefruit peel, coniferous pinus, wheat bran, industrial by-products (Wathukarage *et al.*, 2019), spent mushroom substrate Korean cabbage waste (Sewu *et al*., 2017), ramie stem (Tan *et al.*, 2016), activated carbon, clay minerals, fly ash, acetosolv treated black acacia bark 3D graphene, nanocomposite (Vyavahare *et al.*, 2019).

Removal of lead from water has been widely investigated from diverse materials, i.e. leaf powder of different trees, such as dobera leaves, bael tree, cypress, castor cinchona and pine, neem, rubber, *Cinnamomum camphora* and *Solanum melongena* (Elmorsi *et al.*, 2014). In addition, other materials such as tea leaves (Ahluwalia and Goyal, 2005), tea waste (Amarasinghe and Williams, 2007; Wasewar, 2010), green algae (*Cladophora fascicularis*) (Fu and Wang, 2011), fly ash (Varma *et al*., 2013), iron slag, fly ash from coal-burning (Barakat, 2011), rice husk, walnut, sawdust, peanut husk, banana stem, spent grain, sugarcane bagasse, bagasse, fly ash, sawdust (*Pinus sylvestris*) (Ngah and Hanafiah, 2008), tobacco dust (Qi and Aldrich, 2008) have also been investigated to eliminate lead from water environments.

2.16 Paper mill sludge

Paper mill sludge is generated from the diverse processes of manufacturing paper in pulp and paper industries (Calace *et al.*, 2002). It is estimated that the massive amount of effluent about 20 - 250 m^3/t of air-dried up pulp is formed during paper manufacturing. In addition, disposal of solid, liquid, and suspended matters from the paper manufacturing is about 10 - 400 kg/ton of paper produced (Devi and Saroha, 2014). As a result, the discarding of paper mill sludge has become a waste management issue from these industries (Calace *et al.*, 2002). Furthermore, industrialists and municipal authorities have pressured from regulations and the cost of disposal in addition to the social, political and authorities influence (Wajima, 2014). Therefore, attention has been focused on the possible utilization of paper mill sludge (Calace *et al.*, 2002).

Landfilling, converting to fertilizer, sea dumping and incineration are the conventional disposal methods for paper mill sludge. However, these methods can cause water, air, and soil pollution (Gorzin and Abadi, 2018; Wajima, 2014). In construction fields, the use of paper mill sludge for manufacturing building products has been limited because of uncertainty of market for these products and high capital costs (Calace *et al.*, 2003). Moreover, composting from paper mill sludge is also limited owing to a great amount of C:N ratio (Méndez *et al.*, 2009). However, recycling and rising of paper mill sludge are investigated as alternative methods for the disposal of paper mill sludge. In addition, paper mill sludge has been used for making bricks, agriculture, forestry, and land reclamation (Calace *et al.*, 2003; Devi and Saroha, 2014).

Paper mill sludge which consists of carbonaceous and lignocellulose raw materials (Gorzin and Abadi, 2018) contains a high amount of organic matter and less phosphorus and nitrogen (Méndez *et al.*, 2009). The composition of paper mill sludge shows that it is relatively free of chemical pollutants such as heavy metals and organic pollutants (Calace *et al.*, 2003). However, it contains an excessive concentration of inorganic forms such as Ca and Fe species, generated from the chemical treatment process (Yoon *et al.*, 2017).

Most of the cellulose materials are excellent adsorbents for heavy metal adsorption (Suryan, 2012). Therefore, paper mill sludge can be applied to remove heavy metals from water (Calace *et al.*, 2003). Furthermore, literature has reported that paper mill sludge has been utilized to clear out hazardous dyes from contaminated effluent water (Nargawe *et al.*, 2018).

2.17 Biochar

The investigations of novel adsorbent materials have been boosted in recent years due to the high operational cost for the manufacturing of activated carbon. Therefore, attention has been focused on the production of biochar (Wathukarage *et al.*, 2019). Biochar is a carbon-rich residue generated from the pyrolysis process under oxygen-limited conditions (Ahmad *et al*., 2018; Inyang and Dickenson, 2015; Inyang *et al*., 2016; Oliveira *et al*., 2017; Tan *et al.*, 2016; Vyavahare *et al.*, 2019). In addition, it contains oxygen, nitrogen, hydrogen, and sulfur (Mohan *et al*., 2014). Biochar is a net negative surface charge material due to the dissociation of functional groups on its surface. So, the positive-charged pollutants can be attracted to the adsorbent surface (Vyavahare *et al.*, 2019).

It is observed that different types of feedstock materials have been used in the production of biochar (Yi *et al*, 2015). Biowaste materials such as agriculture waste, forest residue, animal

manure (Sewu *et al*., 2017), activated sludge, algal biomass and energy crops are widely used to produce biochar (Oliveira *et al*., 2017). Biochar is a cost-effective, eco-friendly material in addition to the simple synthesis process (Inyang and Dickenson, 2015). Depending on operational time and temperature, the pyrolysis method can be categorized as slow pyrolysis (350 - 550 °C) and fast pyrolysis (550 - 900 °C) (Mohan *et al*., 2014). The adsorption capacity depends on the pyrolysis conditions: time, temperature, and the chemical composition of biomass (Vyavahare *et al.*, 2019).

The thermochemical process of biomass has energy regaining potential (Tan *et al.*, 2016). In the production process of biochar, cellulose, lignin, fat, hemicellulose and starch are broken down while generating three key products: biochar (solid fraction), bio-oil (partially condensed the volatile matter), non-condensable gases such as CH_4, CO_2, CO (Oliveira *et al*., 2017; Tan *et al.*, 2016). Feedstock type and method of production can alter the chemical properties of biochar. Surface chemistry determines the adsorption mechanism and adsorption capacity of the biochar adsorbent (Lonappan *et al*., 2018). The physical and chemical properties of the sorbates determine the interaction of biochar with organic sorbates. The biochar produced from slow pyrolysis (i.e. below 600 °C) may preserve their parent feedstock chemistry. On the other hand, when pyrolysis temperature increases above 600 °C, carboxylic acids and phenol belonged to aliphatic groups can be transformed to fused basic aromatic groups or neutral (Inyang *et al*., 2015).

Biochar has shown numeric merits, i.e. high specific surface area, extraordinary adsorption capacity, microsporocyte, and ion exchange capacity (Ahmad *et al*., 2018). Biochar has been identified as an alternative adsorbent in wastewater and water treatment processes for controlling diverse pollutants (Sewu *et al.*, 2017). It has been reported that the adsorption capacity of biochar is 10 - 1000 times higher than the other carbon adsorbents (Devi and Saroha, 2015).

Agrochemicals, antibiotics, industrial chemicals, aromatic dyes, polycyclic aromatic hydrocarbon, and volatile organic composites are the common removable organic pollutants by biochar (Oliveira *et al*., 2017; Yi *et al*., 2015). In addition to the remediation methods, biochar can be used for improving the physical, chemical, and biological properties of soil. Also, biochar can be used for carbon sequestration and the reduction of greenhouse gas emissions (Oliveira *et al*., 2017; Sewu *et al*., 2017).

The surface area and porosity of sludge-based biochar are lower than activated carbon. Nonetheless, the biochar's adsorption capacity for an organic pollutant is similar or higher than activated carbon. This phenomenon can be attributed to the occurrence of mineral-rich carbon parts in sludge-based biochar (Devi and Saroha, 2015a). The utilization of biochar for removing dyes is regarded as a green and sustainable method, which can be used as a treatment solution for contaminated groundwater (Tan *et al.*, 2016). By using different solvents, biochar can be reused after the desorption of dye (Vyavahare *et al.*, 2019). The biochar showed promising results for eliminating metallic pollutants namely copper, lead, nickel, and cadmium in the wastewater treatment applications (Inyang *et al.*, 2012).

2.18 Adsorption Isotherms

Adsorption isotherm is an indispensable curve that illustrates the phenomenon governing the retention or mobility of a substance from the aquatic environments or aqueous medium to a solid phase, at a constant pH and temperature (Foo and Hameed, 2010).

Equilibrium studies provide the capacity of an adsorbent and the equilibrium connection between an adsorbate and an adsorbent through adsorption isotherms. In environmental aspects, adsorption isotherms illustrate how pollutants interrelate with adsorbent materials. Therefore, adsorption isotherm studies are important for optimization of the adsorption process, expression of the surface properties and capacities of adsorbents, and the effective design of the adsorption systems. The equilibrium attained in adsorption is demonstrated by plotting the solute amount adsorbed per unit weight of the adsorbent; q_e, versus the solute concentration remained in the solution; C_e (Foo and Hameed, 2010).

The most familiar isotherm models used to characterize adsorbate-adsorbent interactions in batch adsorption studies are the Freundlich and Langmuir models (Febrianto *et al*., 2009; Peric *et al*., 2004). According to the equation of mass balance, the capacity of an adsorbent determines the quantity of ions that is adsorbed onto the adsorbent. Some of the key factors affecting the adsorption capacity can be categorized as the dose of adsorbent, contact time, pH, temperature, and original concentration (Febrianto *et al*., 2009).

2.18.1 Langmuir isotherm model

The Langmuir isotherm explains quantitatively the creation of a monolayer adsorption on the adsorbent outer surface, and after that, no further adsorption occurs on the surface of the

adsorbent (Dada *et al*., 2012). Thus, the equilibrium dispersal of ions among the liquid and solid phases is represented by the Langmuir adsorption isotherm (Vermeulan *et al*., 1966).

The Langmuir isotherm model is applicable only under the given context defined as the assumptions of the Langmuir model. Accordingly, monolayer adsorption is taken onto the surface having a limited number of identical sites (Febrianto *et al*., 2009). Furthermore, even energies of adsorption onto the surface and no transmigration of adsorbate in the surface plane are considered (Kalavathy *et al*., 2005).

The Langmuir isotherm model is stated as:

$$q_e = \frac{q_{max} K_L C_e}{1 + K_L C_e} \tag{2.1}$$

The linearized form of this model can be given as:

$$\frac{C_e}{q_e} = \frac{C_e}{q_{max}} + \frac{1}{K_L q_{max}} \tag{2.2}$$

where, q_e is the solid phase adsorbate concentration at the equilibrium (mg/g), q_{max} is maximum adsorption capacity (mg/g), K_L is the Langmuir constant (L/mg) and C_e is concentration of adsorbate in solution at equilibrium (mg/L). Consequently, isotherm constants for the model can be calculated using the graph plotted with C_e/q_e against C_e (Hameed *et al*., 2007). Thus, the adsorption capacity for target pollutants can be calculated.

2.18.2 Freundlich isotherm model

Freundlich isotherm illustrates the reversible and non-ideal adsorption which is not confined to the monolayer formation. This experiential model can be used to describe multilayer adsorption, with uneven dispersal of adsorption heat, and connecting over the heterogeneous surfaces. This model explains that the quantity adsorbed is the totality of adsorption on the whole sites. In this process, the powerful binding sites are engaged in first, until the adsorption energy is greatly declined upon the fulfillment of the adsorption process (Foo and Hameed, 2010).

The Freundlich equation is an experimental equation engaged to illustrate heterogeneous systems, which is described by the heterogeneity factor *1/n*. Hence, the Freundlich isotherm model is stated as

$$q_e = K_F C_e^{\frac{1}{n}} \quad (2.3)$$

The linear form of this equation is given as

$$\log q_e = \log K_F + \frac{1}{n} \log C_e \quad (2.4)$$

where, q_e is the solid phase adsorbate concentration at the equilibrium (mg/g), C_e is the liquid phase concentration at the equilibrium (mg/L), K_F is the Freundlich adsorption constant (mg/g)(L/mg)$^{1/n}$ and *1/n* is a heterogeneity factor. Therefore, a plot of log q_e versus log C_e enables the constant K_F and exponent *1/n*, an indicator of adsorption effectiveness to be determined (Hameed *et al*., 2007).

2.19 Adsorption kinetics

Kinetic experiments of adsorption are generally performed to determine the time, which is needed to attain the maximum adsorbing capacity of the adsorbate on the adsorbent (Jung *et al*., 2015). It can also be described as the solute elimination rate which governs the residence time of the sorbate in the interface of solid and solution (Febrianto *et al*., 2009).

Febrianto *et al*. (2009) has also mentioned that kinetic experiments are conducted in batch with different types of parameters: temperatures, agitation speeds, particle size, pH values and various types of sorbent and sorbate. The linear regression is applied to establish the best fitting the equation of kinetic rates, such as pseudo-first order, pseudo-second order, Elovich and diffusion kinetic models. Pseudo second order and pseudo first order kinetic models are the most suitable models to explore the adsorption kinetics (Febrianto *et al*., 2009).

The process of liquid/solid adsorption comprises three steps as (i) mass transfer through the external boundary layer film of liquid surrounding the outside of the particle (i.e. external diffusion or film diffusion); (ii) adsorption and desorption among the active sites and adsorbate (i.e. mass action); (iii) diffusion of adsorbate molecules to an adsorption site, either by a pore diffusion process through the liquid filled pores or by a solid surface diffusion mechanism (i.e. intra-particle diffusion) (Cheung *et al*., 2007; Qiu *et al*., 2009). The kinetic adsorption process is always regulated by intra-particle diffusion or liquid film diffusion due to insignificance of mass action process which is owned by a rapid process in physical adsorption. Hence, models

of adsorption kinetics are principally built up to illustrate the process of film diffusion and/or intra-particle diffusion (Qiu *et al*., 2009).

3 AIMS OF THE WORK

The main aim of this research is to evaluate the removal efficiency of Pb(II) and Crystal violet dye from water using biochar, produced from paper mill sludge. To achieve this aim, various laboratory experiments as follows were conducted to optimize the process.

I. The effect of solution pH, adsorbent dosage, contact time, initial concentration and ionic strength for Pb(II) and Crystal violet adsorption were studied and optimized.
II. Langmuir and Freundlich isotherm models were applied to the experimental data, in order to evaluate the adsorbent and adsorbate interaction mechanism at variable initial concentrations and to calculate the maximum adsorption capacity of adsorbents used in this work.
III. Different kinetic models namely pseudo-first order, pseudo-second order and intraparticle diffusion model were studied to understand the rate and mechanism of adsorption.

4 MATERIALS AND METHODS

4.1 Materials

Standard aqueous solutions of Pb(II) and Crystal violet were prepared using an analytical grade reagents of $Pb(NO_3)_2$ (purity > 99%) and $C_{25}H_{30}ClN_3$, respectively. NaCl solution was prepared using NaCl powder (purity ≥ 99%). Solutions of different initial pH were adjusted using 0.1 M HCl and 0.1 M NaOH. Paper mill sludge biochar, used as the adsorbent, was obtained from South Korea. Milli-Q water was used for all experiments.

4.2 Sample preparation

Paper mill sludge (PMS) was obtained from Moorim Paper, Korea. The PMS was oven-dried at 60 °C for 24 hours and then heated by a muffle furnace (LT, Nabertherm, Germany) in a sealed Alumina crucible. The peak temperature was set to 300, 500, and 700 °C at a ramp of 7 °C/min and kept for 2 hours. Finally, samples were named as PSK 300, PSK 500 and PSK 700.

4.3 Batch adsorption studies

Batch adsorption studies were carried out to examine the influence of various experimental parameters. In these experiments, the effect of solution pH, dose, contact time, initial concentration and ionic strength were studied to determine the optimum removal efficiency of Pb(II) and Crystal violet from water. All agitations were done on a roller shaker (IKA® ROLLER) with 50 mL of tubes. All suspensions were filtered through cellulose acetate membrane filters (pore size 0.45 µm, Sartorius, Gmbh Germany). The concentration of Pb(II) ions was measured using Agilent's Microwave Plasma-Atomic Emission Spectrophotometer (4210 MP-AES) and concentration of Crystal violet was measured from UV-VIS spectrophotometer (UV-2401PC). All experiments were conducted at room temperature (25 °C).

4.3.1 Removal percentage and adsorption capacity

Known weight (0.005 g) of biochar samples were added to 50 mL of 20 ppm Pb(II) and Crystal violet solutions. Each sample was agitated at 80 rpm for 24 hours. Then, the suspensions were filtered, and the final concentrations of Pb(II) and Crystal violet were measured. The removal percentage was calculated using the following Equation (4.1):

$$\text{Percentage removal} = \frac{C_i - C_f}{C_i} \times 100 \quad (4.1)$$

where,

C_i - Initial concentration of the metal or dye in the solution before adsorption

C_f - Final concentration of the metal or dye in the filtrate after adsorption

The adsorption capacity was calculated using the following equation (4.2):

$$\text{Adsorption capacity} = \frac{(C_i - C_e)V}{m} \quad (4.2)$$

where,

C_i- Initial concentration of the metal or dye in the solution before adsorption

C_e - Concentration of the metal or dye at the equilibrium

m = adsorbent dose

v = Volume of solution

The concentrations of C_i and C_f were determined by referring to the calibration curve. For the sample concentrations which were not in the linear dynamic range (LDR), necessary dilutions were carried out and the appropriate dilution factors were sonsidered for calculations. All experiments were carried out in duplicate and average values were reported.

4.3.2 Effect of initial solution pH

Effect of initial solution pH for the removal of Pb(II) and Crystal violet was studied over a range of pH 2.0 - 8.0. The desired pH was adjusted by using 0.1 M HCl or 0.1 M NaOH solutions. Adsorbent dosage of 0.005 g and 50 mL of 20 ppm Pb(II) and Crystal violet solutions were mixed and agitated at 80 rpm for 24 hours. The suspensions were filtered, and the final concentrations were measured.

4.3.3 Effect of adsorbent dose

Biochar samples were weighted accurately within the range from 0.0025 g to 0.02 g. The solutions pH was adjusted to 5.5 and 7 for Pb(II) and Crystal violet, respectively. Then, 50 mL of 20 ppm Pb(II) and Crystal violet solutions were mixed with the biochar samples separately. Each sample was agitated at 80 rpm for 24 hours. The percentage removal was calculated using equation 4.1 for the determination of the optimum adsorbent dosage for Pb(II) and Crystal violet.

4.3.4 Isotherm studies

Adsorption isotherm of Pb(II) and Crystal violet on biochar samples were determined by mixing 0.005 g of biochar with 50 mL of different concentrations Pb(II) and Crystal violet solutions. The concentration range was from 20 to 200 ppm under optimized contact time and pH conditions. Necessary dilutions were carried out considering the appropriate dilution factors for calculations. The adsorption capacity was calculated as mg/g using equation 4.2. Adsorption mechanism and adsorption capacity were determined from best-fitted isotherm models.

4.3.5 Kinetic studies

The adsorption kinetics of Pb(II) and Crystal on biochar was examined by mixing 0.005 g of biochar with 50 mL of 20 ppm Pb(II) and Crystal violet solutions. Contact time intervals ranged from 15 min to 1440 min. After agitating at 80 rpm, the suspensions were filtered, and the final concentrations were measured. The kinetic mechanism was studied with different kinetic models.

4.3.6 Effect of ionic strength

Different concentrations of NaCl solutions were prepared ranging from 0.1 M to 0.5 M. The effect of ions for the adsorption of Pb(II) and Crystal violet was studied with the 0.005 g of biochar samples mixing with 50 mL of different concentrations of NaCl and 20 ppm Pb(II) and Crystal violet solutions. Experiments were performed under optimized conditions of pH and contact time. After the agitation, the suspensions were filtered, and the final concentrations were measured.

5 RESULTS AND DISCUSSION

5.1 Batch adsorption studies

5.1.1 Effect of initial solution pH

The pH of the aqueous solution is a very important parameter controlling the adsorption process (Aydin *et al*., 2008). Therefore, the effect of free H^+ ion concentration given by pH was examined on the adsorption of Pb(II) at the pH ranging from 2.0 - 8.0. As shown in Fig. 5.1, the removal percentage was less in low pH values. At lower pH, H^+ ions compete with Pb(II) ions for the sorption sites and it hinders and lowers the Pb(II) adsorption. This behavior can be attributed to several factors: (i) competition between free metal cations and H^+ for the active sites of adsorbent, (ii) repulsion between positive charge of the adsorbent and free metal cations, (iii) lower formation of complexes with metal ions due to protonation of surface functional groups (Villaescusa, 2009), and (iv) combination of some of these factors.

The removal percentage of Pb(II) ions has increased rapidly at pH 3.0 - 5.0 for all PSK biochars. It was reached up to 92.6, 99.6 and 98.0% for PSK 300, PSK 500 and PSK 700 biochars, respectively at pH 8.0. It is observed that between pH 5.0 and 6.0, the removal of metal ion has become approximately constant for all PSK biochars. However, at pH > 7.0, removal percentage of Pb(II) ions has increased slightly for PSK 500 and PSK 700 biochars while removal percentage has rapidly increased from 52.2 to 92.6% in PSK 300 biochar. In addition, at pH > 6.0, Pb(II) ions get precipitated due to hydroxide anion. Therefore, the optimum pH range giving maximum adsorption and preventing precipitation of Pb(II) was within 5.0 - 6.0. Comparing three types of PSK biochars, the highest Pb(II) removal percentage (94.4%) was in PSK 700 biochar followed by PSK 500 and PSK 300 biochars (94.0 and 54.7%, respectively) at pH 6.0. Thus, all experiments for Pb(II) were carried out by adjusting the initial solution pH within 5.0 - 6.0. In literature, a similar Pb(II) removal pattern was observed with initial solution pH when using different materials: tea waste (Amarasinghe and Williams, 2007), orange waste (Dhakal *et al*., 2005) and sago waste (Quek *et al*., 1998).

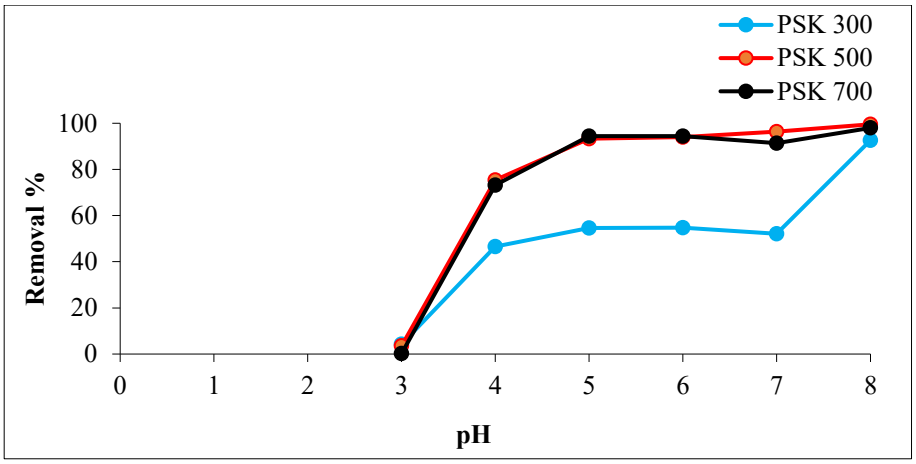

Fig. 5.1: *Effect of pH on Pb(II) removal using PSK biochars (50 mL of 20 mg/L Pb(II) solution, 80 rpm, 24 hours contact time and adsorbent dose = 0.1 g/L).*

According to the Fig. 5.2, the removal percentage of Crystal violet on all three PSK biochar has increased rapidly from pH 3.0 to 6.0. Then, it was reached up to 83.8 and 93.7% for PSK 500 and PSK 700 biochars, respectively at pH 8.0. Beyond pH 6.0, the removal of Crystal violet has become approximately constant for PSK 500 and PSK 700 biochars. However, PSK 300 biochar has shown continuously increased removal percentage from pH 3.0 to 7.0 and reached up to 68.3% at pH 8.0. It is observed that between pH 7.0 and 8.0 there was not significant removal increased on PSK 300 biochar. Comparing three types of PSK biochars, the highest removal percentage was 93.7% from PSK 700 biochar followed by PSK 500 (83.8%) and PSK 300 (68.3%) biochars at pH 7.0. Therefore, pH 7.0 was selected as the best value and all experiments for Crystal violet were conducted in that value. In literature, similar removal pattern was observed for Crystal violet when using different materials: NaOH-modified rice husk (Chakraborty *et al*., 2011) and Gliricidia (Wathukarage *et al.*, 2019).

The solution pH effects on the binding sites of the adsorbent's surface. At lower pH values, functional groups on the adsorbent surface are protonated and the adsorbent surface becomes positively charged. In aqueous solution, Crystal violet dissociates into CV^{+} and Cl^{-} (Chakraborty *et al*., 2011). The high removal percentage of Crystal violet at pH 3.0 to 5.0 can be attributed to the neutralization of negative charge of the adsorbent surface by the positive charge of the cationic dye molecules. However, the high adsorption of Crystal violet at pH 8.0 can be attributed to the electrostatic attraction between positive charge of the dye molecules and negative charge of the adsorbent sites. It is indicated that adsorption is favorable in basic conditions (Mittal *et al.*, 2010).

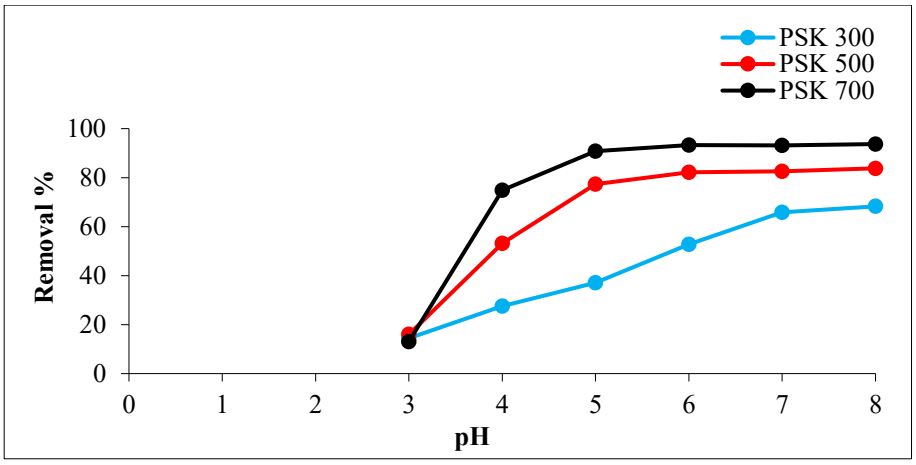

Fig. 5.2: *Effect of pH on Crystal violet removal using PSK biochars (50 mL of 20 mg/L Crystal violet solution, 80 rpm, 24 hours contact time, adsorbent dose = 0.1 g/L).*

5.1.2 Effect of adsorbent dose

The effect of adsorbent's amount is a vital factor in adsorption studies to identify the minimum amount of adsorbent for maximum adsorption of pollutant. The effect of adsorbent dose for the removal of Pb(II) ions is shown in Fig. 5.3. According to the experimental data, the removal percentage of Pb(II) increased for all PSK biochars by increasing the adsorbent dose. This occurs due to the acceleration in the total available adsorption sites and the adsorbent surface area. At the adsorbent dose 0.05 g/L, the lowest Pb(II) removal percentage was observed as 33.8, 70.2 and 63.8% for PSK 300, PSK 500 and PSK 700, respectively. At the adsorbent dose 0.2 g/L, PSK 500 and PSK 700 biochars reached maximum Pb(II) removal percentage (100%) while removal percentage of Pb(II) for PSK 300 biochar was maximum (100%) at an adsorbent dose of 0.4 g/L. It was observed that when increasing the adsorbent dose from 0.005 to 0.01 g the removal percentage of Pb(II) for PSK 700 biochars did not increase significantly. However, significant Pb(II) removal percentage could be observed in PSK 300 and PSK 500 biochars (57 - 92.7% and 82.6 - 100%, respectively from 0.005 to 0.01 g). Similar Pb(II) removal pattern was reported by tea waste when increasing the adsorbent dose (Amarasinghe and Williams, 2007).

When increasing the amount of adsorbent dose, adsorption capacity is decreased. This happens, at the higher adsorbent dose the solution ion concentration falls to a less value and reaching the equlibrum at lower q values (Amarasinghe and Williams, 2007). Therefore, the optimum dose for the removal of Pb(II) was selected as 0.1 g/L for all PSK biochars.

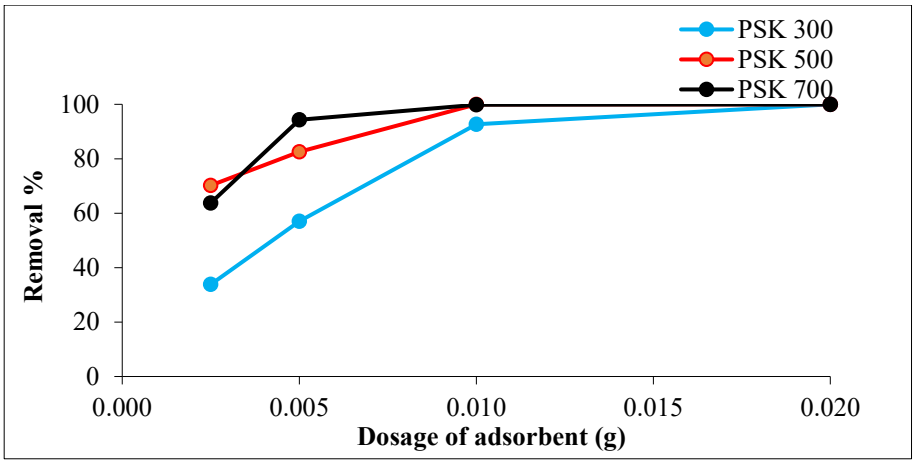

Fig. 5.3: *Effect of adsorbent dose on Pb(II) removal using PSK biochars (50 mL of 20 mg/L Pb(II) solution, 80 rpm, 24 hours contact time and pH= 5.5).*

The effect of adsorbent dose on the removal of Crystal violet is shown in Fig. 5.4. According to the experimental data, the removal percentages of Crystal violet were increased for all PSK biochars by increasing of adsorbent dose. It was observed that by using adsorbent dose of 0.4 g/L, Crystal violet was completely removed (100%) for PSK 500 and PSK 700 biochars. While removal percentage of Crystal violet was 71.8% for PSK 300 biochar at the adsorbent dose 0.4 g/L. It was observed that when increasing adsorbent dose from 0.01 to 0.02 g, removal percentages of Crystal violet for PSK 300 and PSK 700 biochars were almost constant while removal percentage of Crystal violet slightly increased (91.9 - 99.5%) for PSK 500 biochar in that range. Therefore, the optimum dose for the removal of Crystal violet was selected as 0.1 g/L for all PSK biochars.

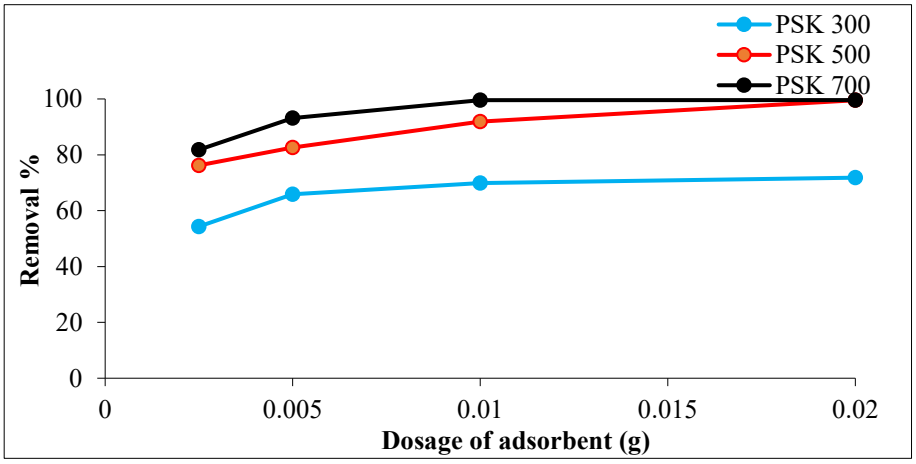

Fig. 5.4: *Effect of adsorbent dose on Crystal violet removal using PSK biochars (50 mL of 20 mg/L Crystal violet solution, 80 rpm, 24 hours contact time, pH = 7.0).*

5.1.3 Effect of ionic strength

Adsorption experiments for the elimination of metals from solution involve sorption and ion exchange mechanisms. For example, sorption of metallic ions by a specific adsorbent may be associated with the solubilization of other ions namely, calcium, sodium, potassium and magnesium (Meunier *et al.*, 2003). According to Fig. 5.5, presence of salt has considerable effect on the adsorption capacity of PSK biochars for Pb(II) which is regulated by the Na^+ and Cl^- ions. By increasing NaCl concentration from 0.1 M to 0.5 M, the adsorption capacity for Pb(II) was decreased by all PSK biochars. The highest adsorption capacities for Pb(II) were 186.5, 177.6, 115.7 mg/g for PSK 700, PSK 500 and PSK 300 biochars, respectively at ionic strength of 0.1 M. The lowest adsorption capacities for Pb(II) were 126.2, 118.7 and 56.4 mg/g for PSK 700, PSK 500 and PSK 300 biochars, respectively at ionic strength of 0.5 M. The difference between the highest and lowest adsorption capacities for Pb(II) were approximately similar for all PSK biochars.

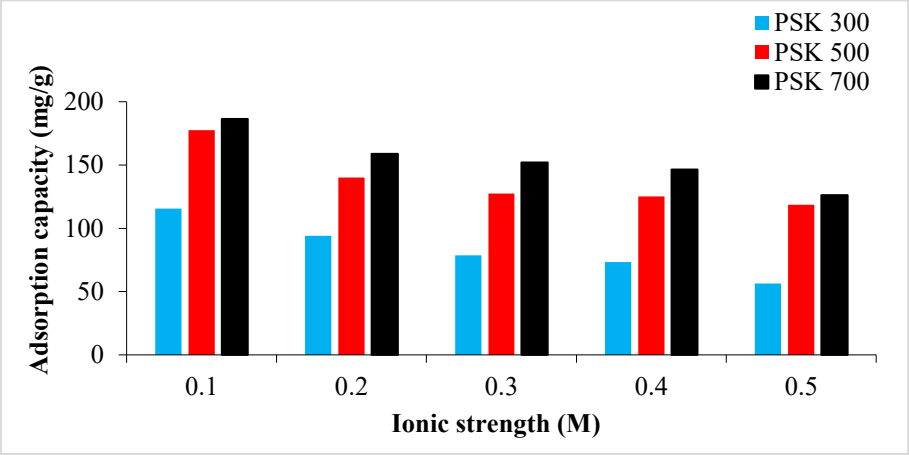

Fig. 5.5: *Effect of ionic strength on Pb(II) removal using PSK biochars (50 mL of 20 mg/L Pb(II) solution, 80 rpm, 24 hours contact time, adsorbent dose = 0.1 g/L and pH = 5.5).*

Dying wastewater generally consists of an excessive amount of salt concentration (Li *et al.*, 2011; Han *et al.*, 2011). So, it is necessary to study the effect of salt concentration on the adsorption of dye. According to Fig. 5.6, when increasing salt concentration from 0.1 M to 0.5 M, adsorption capacity for Crystal violet was decreased by all PSK biochars. The highest adsorption capacities for Crystal violet were 177.5, 158.2, 118.3 mg/g for PSK 700, PSK 500 and PSK 300 biochars, respectively at ionic strengths of 0.1 M. The lowest adsorption capacities for Crystal violet were 156.7, 145.1 and 90.6 mg/g for PSK 700, PSK 500 and PSK 300 biochars, respectively at ionic strength of 0.5 M.

Two possible reactions could have happened during adsorption process when increasing NaCl concentration: (1) NaCl could hinder the electrostatic interaction between Crystal violet cations and functional groups of the adsorbent surface, reducing adsorption capacity; (2) ions could enhance the electrostatic interaction between Crystal violet cations and groups of the adsorbent surface as a result of protonation of Crystal violet molecules (Tan *et al.*, 2016). It was observed that NaCl may release the Na^+ ions which may cover the electrostatic interaction of opposite charges of the adsorbent surface-active sites and Crystal violet molecules. As a result, adsorption capacity for Crystal violet should reduce with increasing ionic strength. In literature, a similar adsorption pattern was reported for Crystal violet from modified Ramie stem biochar (Tan *et al.*, 2016).

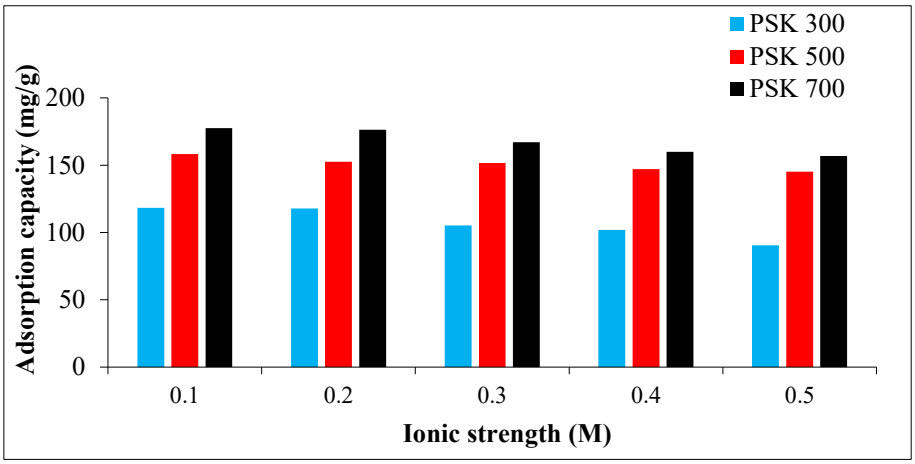

Fig. 5.6: *Effect of ionic strength on Crystal violet removal using PSK biochars (50 mL of 20 mg/L Crystal violet solution, 80 rpm, 24 hours contact time, pH= 7.0, adsorbent dose = 0.1 g/L).*

5.1.4 Isotherm studies

5.1.4.1 Isotherm studies of Pb(II) removal

It is observed (Fig. 5.7) that by increasing of initial Pb(II) ion concentration, the amount of adsorbed Pb(II) ion was increased for all three types of biochars from 112.75 to 179.50 mg/g for PSK 300, from 193.85 to 463.50 mg/g for PSK 500 and from 194.30 to 387.00 mg/g for PSK 700 biochar. Adsoprtion capacities of PSK 700 and PSK 500 biochars have fluctuated up to the Pb(II) ion concentration 150 mg/L. However, adsorption capacities of PSK 700 and PSK 500 biochars have increased continuously after the Pb(II) ion concentration 150 mg/L. All three biochars have shown low adsorption capacites in low Pb(II) concentration values. On the otherhand, high adsorption capacities have displayed when increasing Pb(II) ion concentration.

Among all three biochars the highest adsorption capacity for Pb(II) was in PSK 500 and lowest adsorption capacity was in PSK 300.

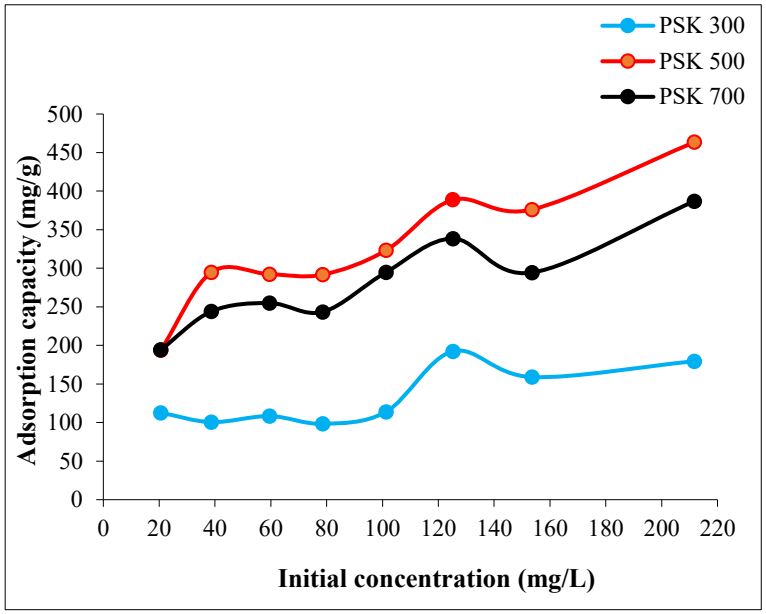

Fig. 5.7: *Effect of initial concentration on Pb(II) removal using PSK biochars (50 mL of Pb(II) solution, 80 rpm, 24 hours contact time, adsorbent dose = 0.1 g/L and pH= 5.5).*

5.1.4.2 Isotherm studies on Crystal violet

As illustrated Fig. 5.8 when increasing the initial Crystal violet concentration, the amount of Crystal violet adsorbed increased for all three types of biochars from 138.51 to 479.22 mg/g for PSK 300, from 158.10 to 798.04 mg/g for PSK 500 and from 178.10 to 938.88 mg/g for PSK 700 biochar. The driving force of the adsorption depends on the solute concentration gradient between the adsorbate and the adsorbent. At lower concentrations, Crystal violet adsorption was much hard due to lower concentration gradient of Crystal violet ions between biochar and the solution. On the other hand, higher Crystal violet concentration has increased the Crystal violet removal through increasing the driving force (Wathukarage *et al.*, 2019).

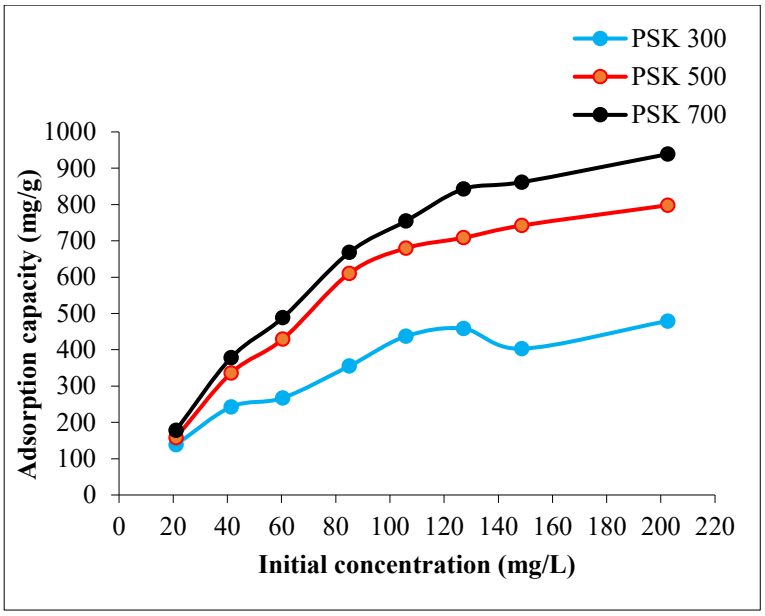

Fig. 5.8: *Effect of initial concentration on Crystal violet removal using PSK biochars (50 mL of Crystal violet solution, 80 rpm, 24 hours contact time, pH= 7.0, adsorbent dose = 0.1 g/L).*

Adsorption isotherms are essential to describe how the adsorbates interact with the adsorbent. Isotherms further provide an idea of the adsorption capacity of the adsorbent where the surface phase may be monolayer or multilayer (Salleh *et al*., 2011). Several equilibrium models have been used to illustrate adsorption isotherm relationships (Amarasinghe and Williams, 2007). With this understanding, the Langmuir and the Freundlich adsorption isotherm models were used to get insight into the adsorption behavior of Pb(II) and Crystal violet by biochar.

5.1.4.3 The Langmuir adsorption isotherm of Pb(II)

Langmuir isotherm model initially has been proposed for adsorption of gases onto solids. However, in liquid-solid systems, the linear form of Langmuir adsorption isotherm can be used (Amarasinghe and Williams, 2007). Langmuir adsorption isotherm is mainly applied for the chemisorption process (Foo and Hameed, 2010). In addition, Langmuir based models are developed for weak physical sorption (Inyang *et al*., 2012). The Langmuir adsorption isotherm (Equation 2.1) is based on three assumptions: (1) adsorption is restricted to monolayer coverage, (2) all surface sites are similar and only one site can hold one adsorbed atom and (3) the capability of a molecule to be adsorbed on a given site is independent of its nearby sites occupancy (Febrianto *et al*., 2009).

The linear form of the Langmuir adsorption isotherms was plotted between C_e vs C_e/q_e according to Equation 2.2 and is shown in Figures 5.9, 5.10 and 5.11 for PSK 300, PSK 500 and PSK 700 biochars, respectively.

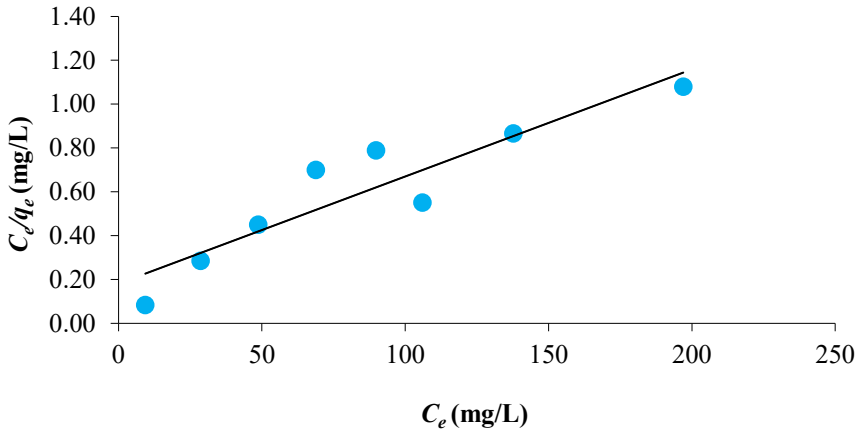

Fig. 5.9: *Langmuir adsorption isotherms for the Pb(II)-PSK 300 biochar system at optimized conditions (50 mL of different initial concentrations of Pb(II) solution, pH 5.5, 80 rpm, 24 hours contact time and adsorbent dose = 0.1 g/L)*

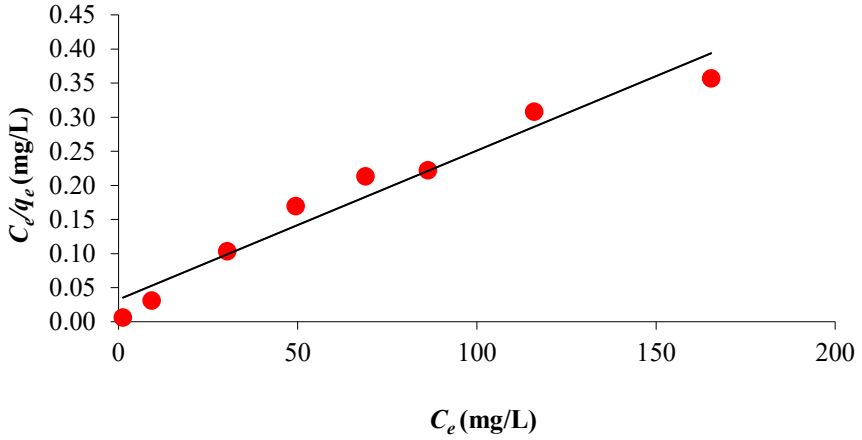

Fig. 5.10: *Langmuir adsorption isotherms for the Pb(II)-PSK 500 biochar system at optimized conditions (50 mL of different initial concentrations of Pb(II) solution, pH 5.5, 80 rpm, 24 hours contact time and adsorbent dose = 0.1 g/L)*

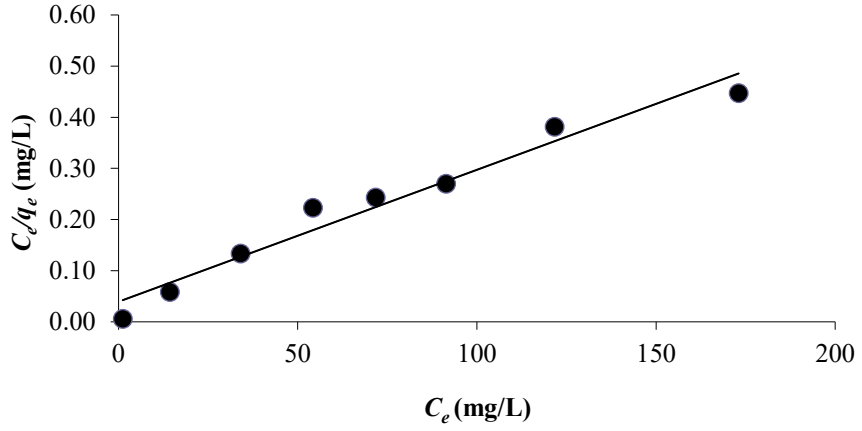

Fig. 5.11: *Langmuir adsorption isotherms for the Pb(II)-PSK 700 biochar system at optimized conditions (50 mL of different initial concentrations of Pb(II) solution, pH 5.5, 80 rpm, 24 hours contact time and adsorbent dose = 0.1 g/L).*

The analyzed data for Langmuir isotherm parameters include Langmuir constant (K_L), the monolayer saturation capacities (q_{max}), regression coefficients (R^2) and the dimensionless

separation factor (R_L) for PSK 300, PSK 500 and PSK 700 (Table 5.1). It is observed that maximum adsorption capacity (q_{max}) was 454.55 mg/g on PSK 500 biochar, showing the highest value among all three types of biochars. The maximum adsorption capacity was 204.08 mg/g on PSK 300 biochar, implying the lowest value compared to the other biochar samples.

The highest value of R^2 was 0.961 on PSK 700 biochar followed by 0.955 and 0.850 for PSK 500 and PSK 300 biochars, respectively, indicating that adsorption data would follow Langmuir equation. The Langmuir isotherm signifies the homogeneous distribution of energetic sites throughout the biochar particle surface. The fitness of the Pb(II) concentration data to the Langmuir isotherm for PSK 300, PSK 500 and PSK 700 biochars is indicative of monolayer coverage of Pb(II) on the homogeneous biochar surface with no interactions between the adsorbed molecules (Amarasinghe and Williams, 2007). In literature, monolayer capacities for the adsorption of Pb(II) were reported as 104.00, 83.00 and 33.78 mg/g on Bael leaves, Dobera leaves and electric furnace slag, respectively (Elmorsi *et al.*, 2014). Thus, the obtained data indicates that PSK 300, PSK 500 and PSK 700 biochars could be considered as efficient adsorbents for Pb(II) removal when comparing with some other adsorbents.

Table 5.1: *Isotherm parameters, separation factor (R_L) and regression coefficient (R^2) for the Langmuir isotherm model for Pb(II).*

Type	K_L (L/mg)	q_{max} (mg/g)	R^2	$R_{L\ avg}$
PSK 300	0.027	204.08	0.850	0.375
PSK 500	0.068	454.55	0.955	0.191
PSK 700	0.066	384.62	0.961	0.220

The key characteristics of the Langmuir isotherm can be illustrated by the dimensionless separation factor; R_L, as defined by the following equation (Wasewar, 2010).

$$R_L = \frac{1}{1+K_L C_i} \tag{5.1}$$

where, C_i is the initial concentration of metal ions and K_L is the Langmuir constant. The value of R_L indicates the nature of adsorption isotherms to be unfavorable ($R_L > 1$), linear ($R_L = 1$), favorable ($R_L < 1$) or irreversible ($R_L = 0$) (Wasewar, 2010). Therefore, for all three types of biochars, the favorability of the adsorption process supports by the average R_L values as given in Table 5.1. According to data, R_L values were 0.375, 0.191 and 0.220 for PSK 300, PSK 500 and PSK 700 biochars, respectively which were below the value of one. Therefore, the nature

of adsorption isotherm for all three biochars should be favorable and all are good adsorbents for Pb(II) adsorption. Comparing all three biochars, PSK 500 biochar has shown the best performance for adsorption of Pb(II), considering maximum adsorption capacity (454.55 mg/g) and lowest separation factor (0.191).

5.1.4.4 The Langmuir adsorption isotherm of Crystal violet

The linear form of the Langmuir adsorption isotherm was plotted between C_e vs C_e/q_e according to Equation 2.2 and is shown in Figures 5.12, 5.13 and 5.14 for PSK 300, PSK 500 and PSK 700, respectively.

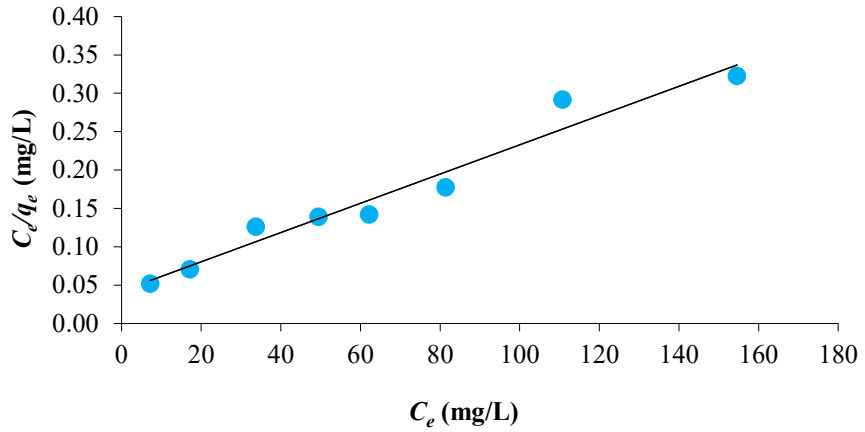

Fig. 5.12: *Langmuir adsorption isotherms for the Crystal violet-PSK 300 biochar system at optimized conditions (50 mL of different initial concentrations of Crystal violet solution, pH 7.0, 80 rpm, 24 hours contact time, adsorbent dose = 0.1 g/L).*

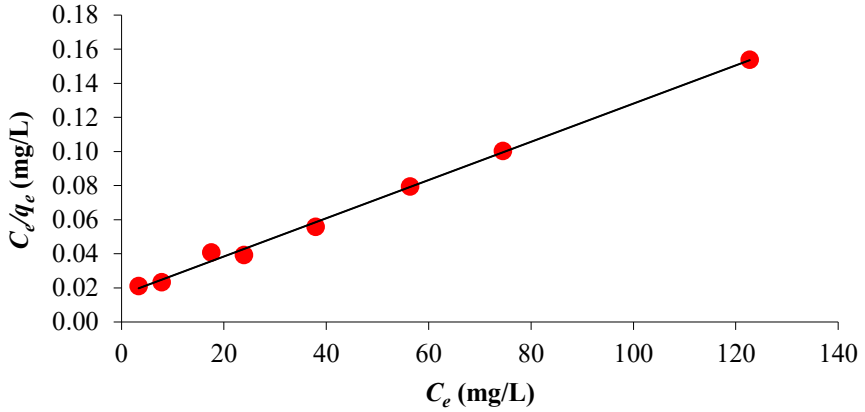

Fig. 5.13: *Langmuir adsorption isotherm for the Crystal violet-PSK 500 biochar system at optimized conditions (50 mL of different initial concentrations of Crystal violet solution, pH 7.0, 80 rpm, 24 hours contact time, adsorbent dose = 0.1 g/L).*

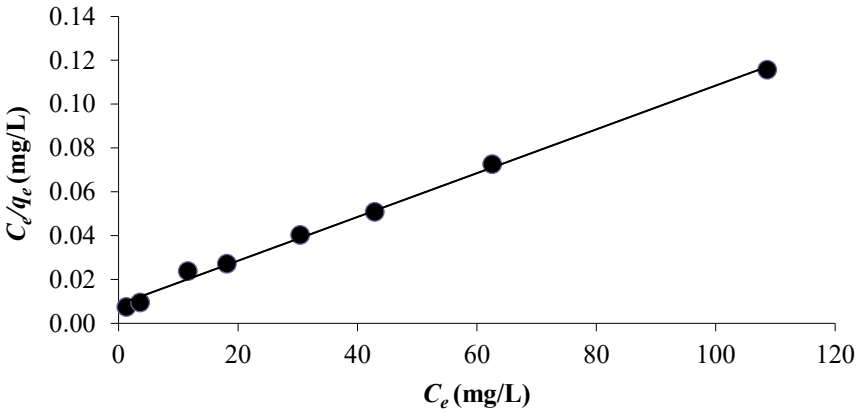

Fig. 5.14: *Langmuir adsorption isotherm for the Crystal violet-PSK 700 biochar system at optimized conditions (50 mL of different initial concentrations of Crystal violet solution, pH 7.0, 80 rpm, 24 hours contact time, adsorbent dose 0.1 g/L g).*

The analyzed data for Langmuir isotherm parameters for PSK 300, PSK 500 and PSK 700 biochars are shown in Table 5.2. It is observed that maximum adsorption capacity (q_{max}) was 1000 mg/g on PSK 700 biochar followed by 909.09 and 526.32 mg/g on PSK 500 and PSK 300 biochars, respectively. The values of R^2 were 0.997, 0.996 and 0.957 for PSK 700, PSK 500 and PSK 300 biochars, respectively, indicating that adsorption data is well fitted to the Langmuir equation. It is reported that in literature, monolayer capacities for the adsorption of Crystal violet were 374.69, 271.0 and 282.9 mg/g for biochar produced from Ramie stem (Tan *et al.*, 2016), activated carbon (Sewu *et al*., 2017) and biochar produced from a spent mushroom substrate, respectively (Sewu *et al.*, 2017). Thus, when comparing with some other adsorbents PSK 300, PSK 500 and PSK 700 biochars can be considered as efficient adsorbents for Crystal violet removal.

According to data, R_L values were 0.565, 0.189 and 0.110 for PSK 300, PSK 500 and PSK700 biochars, respectively which were below the value of one. Therefore, the nature of adsorption isotherm for all three biochars should be favorable for Crystal violet adsorption. Comparing all three biochars, PSK 700 biochar shows the best performance for adsorption of Crystal violet, considering maximum adsorption capacity (1000 mg/g), regression coefficients (0.997) and lowest separation factor (0.110).

Table 5.2: *Isotherm parameters, separation factor (R_L) and regression coefficient (R^2) for the Langmuir isotherm model for Crystal violet.*

Type	K_L (L/mg)	q_{max} (mg/g)	R^2	$R_{L\ avg}$
PSK 300	0.045	526.32	0.957	0.565
PSK 500	0.069	909.09	0.996	0.189
PSK 700	0.116	1000.00	0.997	0.110

5.1.4.5 The Freundlich adsorption isotherm on Pb(II) and Crystal violet for PSK biochars

The Freundlich adsorption isotherm (Equation 2.3) describes the surface heterogeneity which signifyies multilayer adsorption on the adsorbent surface. In the Freundlich isotherm, K_F and n can be calculated using the slope and the intercept of the graph, where K_F and n are the Freundlich empirical constants describe sorption capacity and sorption intensity, respectively. If value of $1/n$ is less than 1, it signifies normal adsorption. If n lies between 1.0 and 10.0, it indicates a favorable adsorption process (Dada *et al*., 2012; Febrianto *et al*., 2009). Adsorption intensity or surface heterogeneity determines the slope ranges between 0 and 1. When the value is closer to zero it implies more heterogeneous (Foo and Hameed, 2010). In addition, higher values of n indicate stronger interaction between adsorbent and adsorbate and linear adsorption leading to identical adsorption energies for all sites is given by $1/n = 1$ (Febrianto *et al*., 2009).

From the data in Table 5.3, that value of $1/n$ = 0.177, 0.149 and 0.122, while n = 5.650, 6.711 and 8.197 for PSK 300, PSK 500 and PSK 700, respectively, indicating that the adsorption of Pb(II) onto all three types of biochars has stronger interaction between adsorbent and adsorbate and is favorable at studied conditions. PSK 700 biochar has displayed a more favorable adsorption process for Pb(II) and has strong interactions (n = 8.197) with adsorbate compared to the other two biochars.

From the data in Table 5.4, values of $1/n$ were 0.394, 0.437 and 0.367, while n = 2.538, 2.288 and 2.725 for PSK 300, PSK 500 and PSK 700, respectively which indicate that the adsorption of Crystal violet onto all biochars has strong adsorption intensity and is favorable at studied conditions. Freundlich constant (K_F) displays the degree of adsorption. Increasing K_F values with increasing pyrolysis temperature suggests the adsorption process for Crystal violet is highly favorable for biochar produced at high pyrolysis temperature (Wathukarage *et al.*, 2019). Thus, PSK 700 has shown the highest adsorption capacity (K_F = 194.98 mg/g) for Crystal violet

compared to PSK 300 and PSK 500. In addition, the value of 1/*n* decreases with increasing pyrolysis temperature which confirms the feasibility of adsorption process for PSK 700 biochar (1/*n* = 0.122). A similar observation was reported from biochar produced from Gliricidia sepium (Wathukarage *et al.*, 2019).

5.1.4.6 Selecting the best adsorption isotherm on Pb(II) and Crystal violet

Table 5.3 and 5.4 have shown the constants for Langmuir and Freundlich adsorption isotherm for Pb(II) and Crystal violet, respectively. The magnitude of linear regression coefficient (R^2) is used to find the best-suited adsorption isotherm for Pb(II) and Crystal violet . Therefore, the isotherm which gives the R^2 value closest to unity is taken as the best fit.

Interactions between PSK 300, PSK 500 and PSK 700 biochars with Pb(II) and Crystal violet are found to obey the Langmuir adsorption isotherm better than the Freundlich isotherm, as the regression coefficients of Langmuir model are closer to 1 compared to the Freundlich isotherm in all experiments. It can be assured that the adsorption occurs in a homogeneous manner on the surface of the adsorbate and ions form a monolayer without having transmigration of adsorbate in the plane of surface (Hameed *et al*., 2007). In addition, it is observed that PSK 700 biochar showed the better fit to Langmuir model for Pb(II) and Crystal violet than the other two types of biochars.

Langmuir and Freundlich isotherms adsorption capacities onto various materials for Pb(II) and Crystal violet have been reported in above sections. It is apparent that the PSK biochars used in this study have displayed better adsorption characteristics with respect to other types of adsorbent materials tested in different countries. However, it should be noted that adsorption capacities always heavily depend on different operation conditions.

Table 5.3: *Langmuir and Freundlich adsorption isotherms on Pb(II).*

Type	Pb(II)						
	Langmuir			Freundlich			
	K_L (L/mg)	q_{max} (mg/g)	R^2	n	1/n	K_F (mg/g)(L/mg)$^{1/n}$)	R^2
PSK 300	0.027	204.08	0.850	5.650	0.177	61.659	0.407
PSK 500	0.068	454.55	0.955	6.711	0.149	187.930	0.852
PSK 700	0.066	384.62	0.961	8.197	0.122	178.23	0.794

Table 5.4: *Langmuir and Freundlich adsorption isotherms on Crystal violet.*

Type	Crystal violet						
	Langmuir			Freundlich			
	K_L (L/mg)	q_{max} (mg/g)	R^2	n	$1/n$	K_F (mg/g)(L/mg)$^{1/n}$)	R^2
PSK 300	0.045	526.32	0.957	2.538	0.394	71.610	0.901
PSK 500	0.069	909.09	0.996	2.288	0.437	120.230	0.904
PSK 700	0.116	1000.00	0.997	2.725	0.367	194.98	0.937

5.1.5 Kinetic studies

5.1.5.1 Kinetic studies on Pb(II)

The adsorption capacity for Pb(II) against the contact time is shown in Fig. 5.15. Accordingly, adsorption capacities of Pb(II) on PSK 300, PSK 500 and PSK 700 biochars have reached 78.50, 156.60 and 181.4 mg/g, respectively in 6 hours. The equilibrium was reached in 24 hours. It is observed that adsorption capacities for Pb(II) for all PSK biochars have not significantly increased from 6 hours to 24 hours.

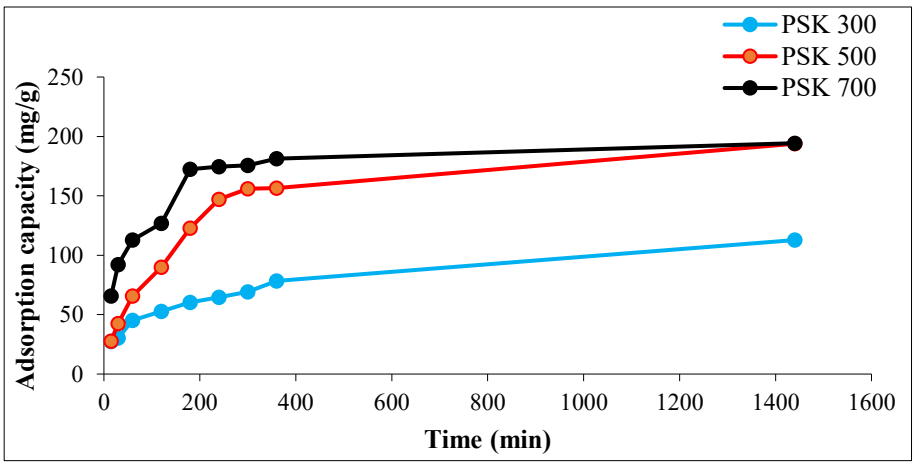

Fig. 5.15: *Effect of contact time on Pb(II) removal using PSK biochars (50 mL of 20 ppm Pb(II)solution, 80 rpm, pH = 5.5 and adsorbent dose = 0.1 g/L).*

Adsorption kinetic models have been applied to describe the behavior of batch biosorption processes (Itodo *et al*., 2010). In kinetic studies, the solute uptake rate will determine the residence time of the adsorption reaction. Generally, the performance of fixed-bed or any other flow-through system is determined basically by the adsorption kinetic (Qiu *et al*., 2009).

Fitting the experimental data into kinetic models can be used to determine the adsorption rate and applicable model of the adsorption process. Also, it helps to forecast the information about adsorbate-adsorbent interactions, chemisorption or physisorption (Elmorsi *et al.*, 2014). Various types of adsorption kinetic models have been used to identify the adsorption kinetics and rate-limiting step (Amarasinghe and Williams, 2007). In this study, pseudo-first order, pseudo-second order and intraparticle diffusion models were applied to determine the kinetics of the system. The generalized equation for kinetics, introduced by Lagergren is expressed as follows (Lagergren, 1898**)**.

$$\frac{d(q_t)}{dt} = k_1\,(q_e - q_t)^n \tag{5.2}$$

where k_1 is the rate constant, t is the contact time, q_e and q_t are amount of adsorbate adsorbed per unit weight of adsorbent at equilibrium and at time t, respectively, and n is the order of the reaction with respect to adsorbate.

The following kinetic models were obtained with the rearrangement of the equation (5.2), and can be expressed for,

Pseudo first order as:

$$log\,(q_e - q_t) = -\frac{k_1}{2.303}t + log\,q_e \tag{5.3}$$

Rearranging the equation (5.2) Pseudo second order model was proposed by Ho and McKay (1999) as:

$$\frac{t}{q_t} = \frac{1}{q_e}t + \frac{1}{(k_2 q_e^{\,2})} \tag{5.4}$$

Further, if the initial adsorption rate is h_o,

$$h_0 = k_2 q_e^2 \tag{5.5}$$

The respective kinetic behaviors for Pb(II), explained by the pseudo first order and pseudo second order kinetic models, are shown in Fig. 5.16, 5.17 for PSK 300, Fig. 5.18, 5.19 for PSK 500 and Fig. 5.20, 5.21 for PSK 700, respectively.

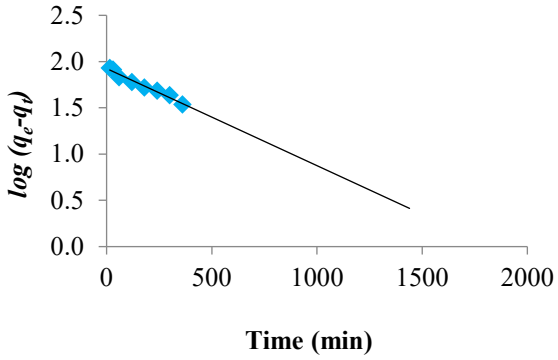

Fig. 5.16: *Pseudo first order kinetic model for the interaction of PSK 300 with 20 ppm Pb(II) solution.*

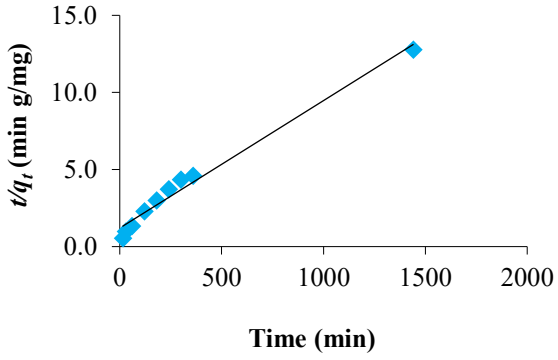

Fig. 5.17: *Pseudo second order kinetic model for the interaction of PSK 300 with 20 ppm Pb(II) solution.*

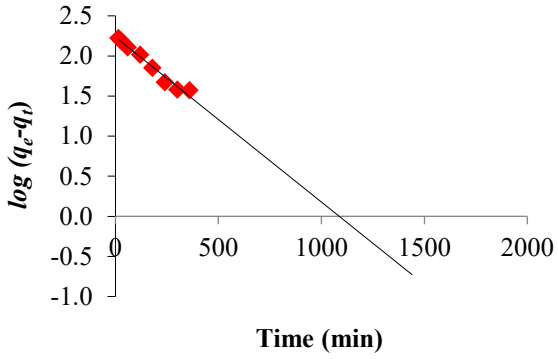

Fig. 5.18: *Pseudo first order kinetic model for the interaction of PSK 500 with 20 ppm Pb(II) solution.*

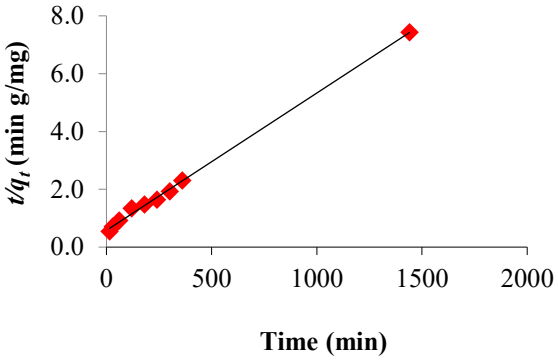

Fig. 5.19: *Pseudo second order kinetic model for the interaction of PSK 500 with 20 ppm Pb(II) solution.*

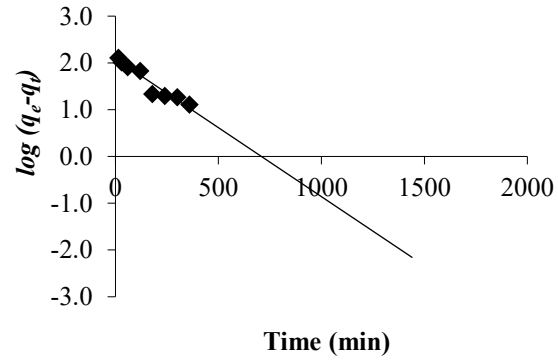

Fig. 5.20: *Pseudo first order kinetic model for the interaction of PSK 700 with 20 ppm Pb(II) solution.*

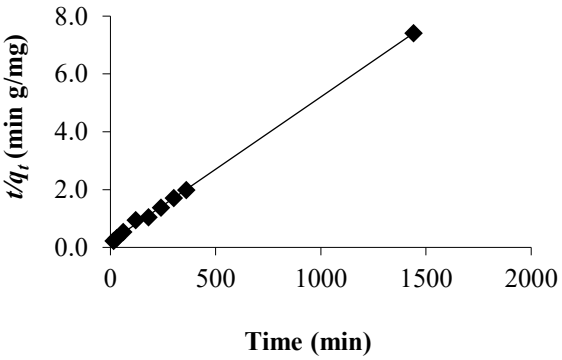

Fig. 5.21: *Pseudo second order kinetic model for the interaction of PSK 700 with 20 ppm Pb(II) solution.*

Kinetic data of Pb(II) for pseudo first order and pseudo second order models is reported in Table 5.5 with the correlation coefficients (R^2). The linear regression coefficient is applied to

determine the best fitting model (Febrianto *et al*., 2009). Adsorption of Pb(II) on to all PSK biochars was not fitted into first order kinetic model since values of R^2 were lower than pseudo second order kinetic model. Thus, pseudo second order model was more appropriate to represent the kinetic data on all three types of biochar-Pb(II) systems having correlations given by R^2 of 0.981, 0.998 and 0.999 for PSK 300, PSK 500 and PSK 700, respectively. This result is supported by literature for the adsorption of Pb(II) onto Dobera leaves (Elmorsi *et al.*, 2014), tea waste (Amarasinghe and Williams, 2007), digested dairy waste biochar (Inyang *et al.*, 2012) and sago waste (Quek *et al*., 1998) in compliance to the pseudo second order kinetics.

5.1.5.2 Kinetic studies on Crystal violet

The adsorption capacity of Crystal violet against the contact time is shown in Fig. 5.22. Accordingly, the equilibrium was reached in 24 hours for all PSK biochar. It is observed that maximum adsorption capacities for PSK 300, PSK 500 and PSK 700 were 138.51, 176.96 and 196.96 mg/g, respectively at equilibrium.

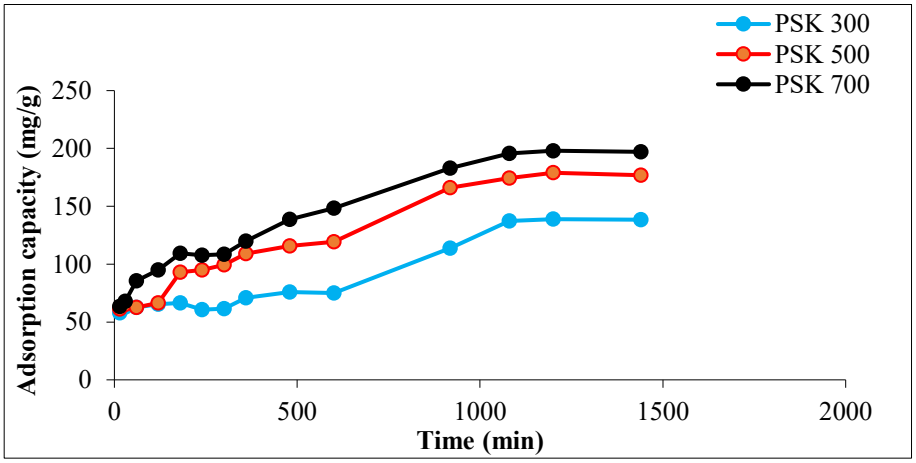

Fig. 5.22: *Effect of contact time on Crystal violet removal using PSK biochars (50 mL of 20 ppm Crystal violet solution, 80 rpm, pH = 7.0, adsorbent dosage = 0.1 g/L).*

The respective kinetic behaviors for Crystal violet explained by the pseudo first order and pseudo second order kinetic models are shown in Fig. 5.23, 5.24 for PSK 300, Fig. 5.25, 5.26 for PSK 500, and Fig. 5.27, 5.28 for PSK 700, respectively.

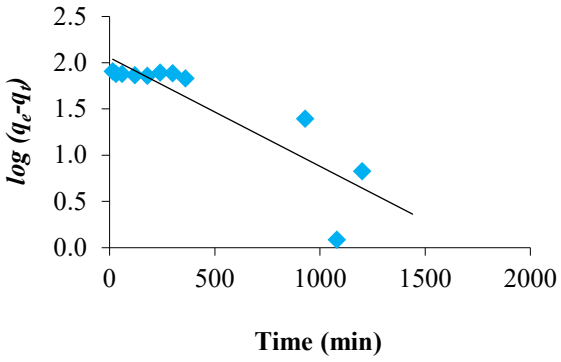

Fig. 5.23: *Pseudo first order kinetic model for the interaction of PSK 300 with 20 ppm Crystal violet solution.*

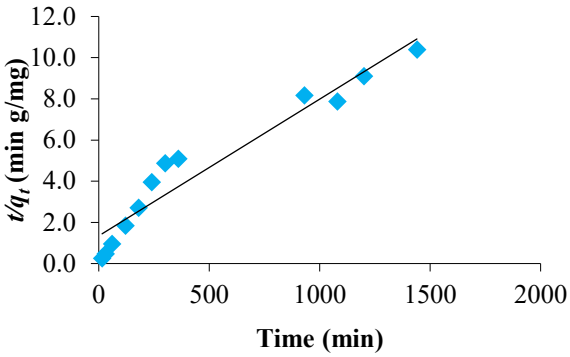

Fig. 5.24: *Pseudo second order kinetic model for the interaction of PSK 300 with 20 ppm Crystal violet solution.*

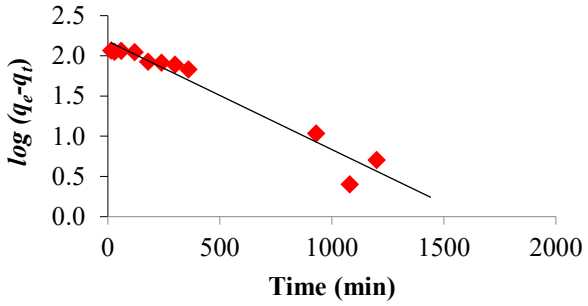

Fig. 5.25: *Pseudo first order kinetic model for the interaction of PSK 500 with 20 ppm Crystal violet solution.*

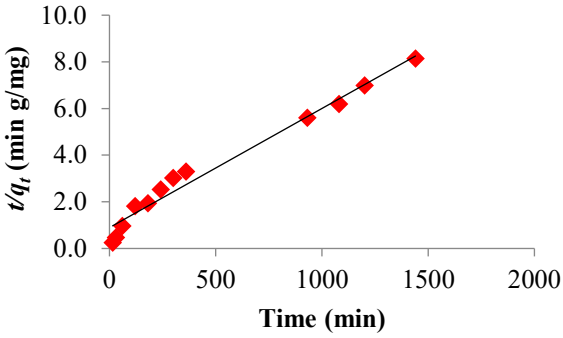

Fig. 5.26: *Pseudo second order kinetic model for the interaction of PSK 500 with 20 ppm Crystal violet solution.*

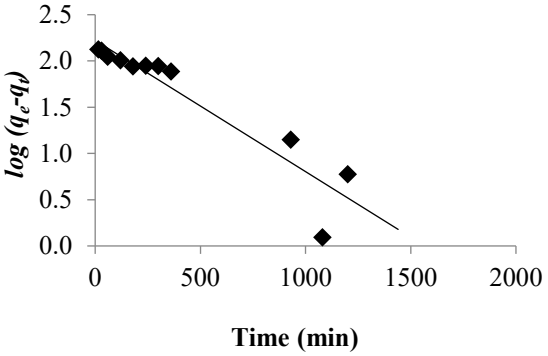

Fig. 5.27: *Pseudo first order kinetic model for the interaction of PSK 700 with 20 ppm Crystal violet solution.*

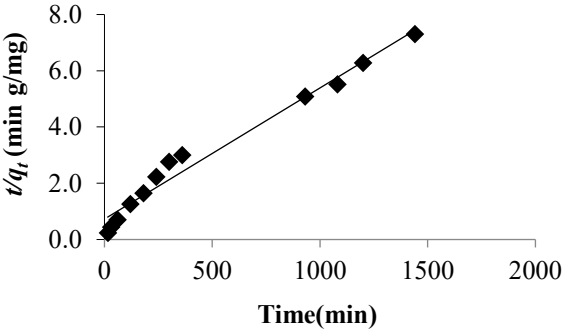

Fig. 5.28: *Pseudo second order kinetic model for the interaction of PSK 700 with 20 ppm Crystal violet solution.*

Kinetic data of Crystal violet for pseudo first order and pseudo second order models is reported in Table 5.6 with the correlation coefficients (R^2). Pseudo first order model was not fitted to all

three types of biochars. However, pseudo second order kinetic model was more appropriate to represent the kinetic data on all PSK biochar-Crystal violet systems with R^2 of 0.930, 0.975 and 0.976 for PSK 300, PSK 500 and PSK 700, respectively. Similar results were reported in the literature by other researchers using different adsorbents (Mittal *et al.*, 2010), (Chakraborty *et al*., 2011) (Wathukarage *et al.*, 2019).

The pseudo second order kinetics model explains that the rate-limiting step of an adsorption mechanism related to the chemisorption process. In this process, valence forces can be involved via sharing or exchanging electrons between the sorbent and the sorbate. In addition, complexation, coordination and/or chelation are possible occurrences that can take place in this process (Febrianto *et al*., 2009). The rate constant also gives a measure of reaction rate and thus, adsorption rate and the initial rate of adsorption (h_o), demonstrate how fast the reaction proceeds. However, the order is determined based on kinetics, which depends on the path to reach equilibrium (Mall *et al*., 2006). The advantage of the pseudo second order model is that it does not have a problem of assigning an effective adsorption capacity, finding the pseudo second order rate constant and the initial adsorption rate thereby all can be determined from the equation without knowing any parameter beforehand (Ho, 2006).

Even though high correlation coefficient is shown in pseudo first order model, the reaction cannot be classified as pseudo first order if they have large difference in experimental q_e value and calculated q_e value (Febrianto *et al*., 2009). In this study, calculated q_e values agreed with experimental q_e values in pseudo second order model than pseudo first order model for Pb(II) and Crystal violet on all PSK materials. Therefore, it is indicated that in addition to the correlation coefficient, pseudo second order model was well fitted with experimental kinetic data.

Table 5.5: *Kinetic parameters given by the pseudo second order model for adsorption of Pb(II) on PSK biochars.*

Type	$q_{e\,cal}$ (mg/g)	$q_{e\,exp}$ (mg/g)	K_2 (g/mg min)	h_o (mg/g min)	R^2
PSK 300	120.482	112.75	5.727×10^{-5}	0.831	0.981
PSK 500	208.333	193.85	3.989×10^{-5}	1.731	0.998
PSK 700	200.000	194.30	1.239×10^{-4}	4.955	0.999

Table 5.6: *Kinetic parameters given by the pseudo second order model for adsorption of Crystal violet on PSK biochars.*

Type	$q_{e\ cal}$ (mg/g)	$q_{e\ exp}$ (mg/g)	K_2 (g/mg min)	h_o (mg/g min)	R^2
PSK 300	151.515	138.51	3.238×10^{-5}	0.743	0.930
PSK 500	196.078	176.96	2.904×10^{-5}	1.116	0.975
PSK 700	212.766	196.96	3.053×10^{-5}	1.374	0.976

5.1.5.3 Intra-particle diffusion modelling

Adsorption reaction models and adsorption diffusion models have been applied to illustrate the kinetic process of adsorption. However, they are extremely dissimilar in nature. The mechanism of adsorption diffusion models involves three steps namely, film diffusion, intra-particle diffusion and mass action. Nonetheless, adsorption reaction models deriving from chemical reaction kinetics are based on the entire process of adsorption, not taking into consideration these three steps stated above (Qiu *et al*., 2009).

Intra-particle diffusion, which has been employed to illustrate the adsorption process taking place on porous adsorbent, is a transport process that involves movement of species from the bulk of the solution to the solid phase. There are several complex mathematical relationships involved in the intra-particle diffusion model and involvement of intra-particle diffusion can be analyzed by using the Weber and Morris equation (5.6) (Itodo *et al*., 2010). Linear behavior of the data describes that the sorption process follows the intra-particle diffusion model and the initial rate of intra-particle diffusion is calculated by this model (Yakout and Elsherif, 2010).

$$q_t = kt^{0.5} + C \qquad (5.6)$$

where, q_t is the amount of ion adsorbed per unit mass of the sorbent at time t, k is the intraparticle diffusion rate constant, mg/g min/$^{0.5}$ and C is the intercept.

According to literature, if intra-particle diffusion is involved in the adsorption process, the plot should be linear, and if these lines pass through the origin then intra-particle diffusion will be the rate-controlling step (Yakout and Elsherif, 2010)**.** The deviation of regression line from the

origin can also be used to describe the differences in the rate of mass transfer in the initial and final stages of adsorption and moreover such deviation of a straight line from the origin indicates that the pore diffusion is not the sole rate-controlling step (Mall *et al*., 2006).

The linear regression coefficient (R^2) values (Table 5.7) obtained by the intra-particle diffusion model plots for Pb(II) and Crystal violet are shown in Figures 5.29, 5.30, 5.31 and 5.32, 5.33, 5.34, respectively. The findings of the current study for Pb(II) and Crystal violet show that the regression lines for all PSK biochars do not pass through the origin thereby rate-controlling would not be governed by intra-particle diffusion only. Further, it describes intra-particle diffusion is not the only rate-limiting step and the rate of adsorption may regulate by the other mechanisms also, functioning simultaneously (Mall *et al*., 2006; Yakout and Elsherif, 2010).

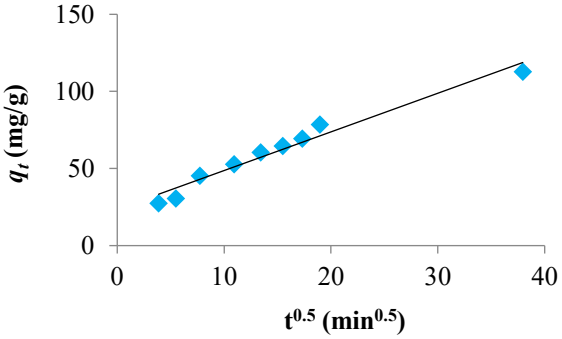

Fig. 5.29: *Intra particle diffusion model for the interaction of Pb(II)-PSK 300 with, 20 ppm Pb(II) solution.*

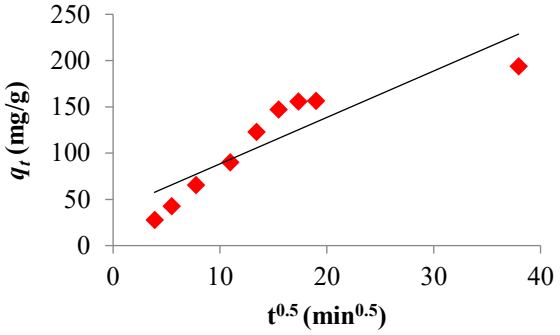

Fig. 5.30: *Intra particle diffusion model for the interaction of Pb(II)-PSK 500 with, 20 ppm Pb(II) solution.*

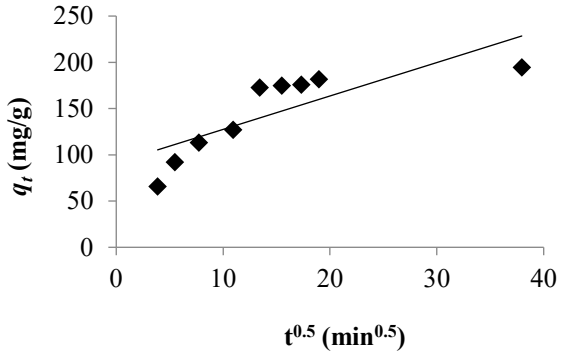

Fig. 5.31: *Intra particle diffusion model for the interaction of Pb(II)-PSK 700 with, 20 ppm Pb(II) solution.*

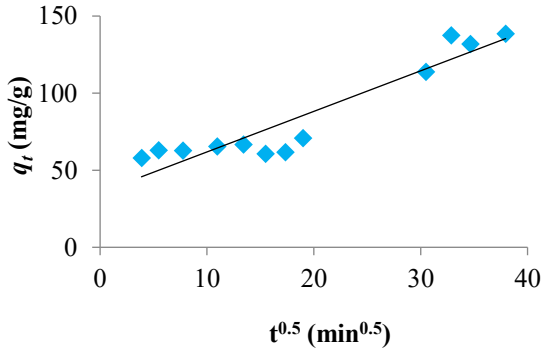

Fig. 5.32: *Intra particle diffusion model for the interaction of Crystal violet-PSK 300 with, 20 ppm Crystal violet solution.*

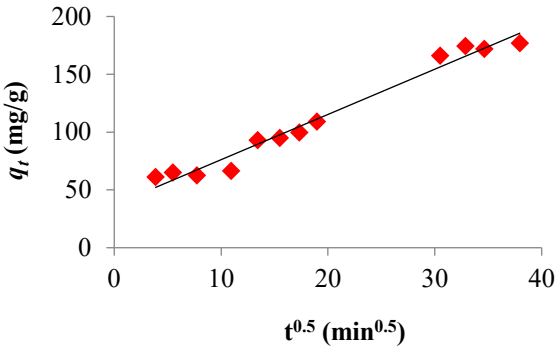

Fig. 5.33: *Intra particle diffusion model for the interaction of Crystal violet-PSK 500 with, 20 ppm Crystal violet solution.*

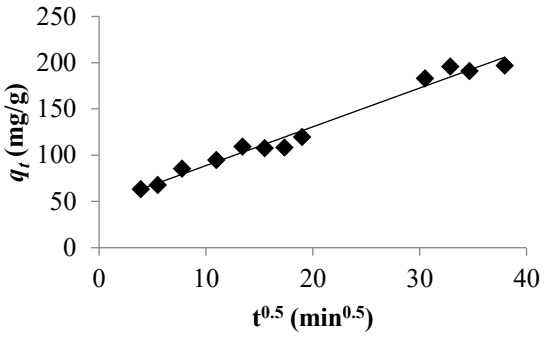

Fig. 5.34: *Intra particle diffusion model for the interaction of Crystal violet-PSK 700 with, 20 ppm Crystal violet solution.*

Table 5.7: *Linear regression coefficients (R^2) for Pb(II) and Crystal violet adsorption on PSK biochars obtained for intra particle diffusion model.*

Type	Pb(II)	Crystal violet
PSK 300	0.964	0.889
PSK 500	0.792	0.975
PSK 700	0.647	0.981

6 CONCLUSIONS AND SUMMARY

Paper mill sludge (a commonly available unavoidable waste material associated with the paper processing industry) is an effective adsorbent when it is converted to biochar which can be used to remove Pb(II) and Crystal violet from water. In this study, various forms of paper mill sludge biochar (PSK 300, PSK 500 and PSK 700) were used to remove the Pb(II) and Crystal violet from water. The characterization of biochar samples was not possible due to lockdown of the university due to COVID-19. The maximum adsorption capacity of Pb(II) and Crystal violet was achieved under optimized conditions. The optimized initial solution pH was found to be 5.5 and 7.0 for Pb(II) and Crystal violet, respectively. The maximum adsorption capacities of biochars were 454.55 mg/g and 1000 mg/g for Pb(II) and Crystal violet, respectively.

The presence of NaCl concentration in the adsorption media for Pb(II) and Crystal violet reduced the adsorption capacity of all biochars. The adsorption process followed the Langmuir adsorption isotherm that favors chemical adsorption processes. The value of $1/n$ in Freundlich model was between 0 and 1, which indicated that the adsorption process of Pb(II) and Crystal violet onto all three PSK biochars was favorable. The sorption kinetics were well described by the pseudo second order kinetic model for Pb(II) and Crystal violet with the highest regression coefficients. The rate constants represented that chemisorption was involved in the adsorption process and revealed that intra-particle diffusion is not the only rate-limiting step of the adsorption process.

Among all three types of PSK biochars, PSK 700 biochar showed the highest performance for the removal of Pb(II) and Crystal violet from water. Adsorbent characteristics proved by PSK biochars can be used to innovate new adsorbents which can be applied in an environment rich in Pb(II) and Crystal violet waste. Furthermore, suitable modifications of the adsorbent could further improve the efficiency of the material.

REFERENCES

Ahluwalia, S.S. and Goyal, D. 2005. Removal of heavy metals by waste tea leaves from aqueous solution. Engineering in life Sciences 5(2): 158-162. doi: 10.1002/elsc.200420066.

Ahmed, M.J. and Hameed, B.H. 2018. Removal of emerging pharmaceutical contaminants by adsorption in a fixed-bed column: a review. Ecotoxicology and environmental safety 149: 257-266. doi: 10.1016/j.ecoenv.201.

Alshabanat, M., Alsenani, G. and Almufarij, R. 2013. Removal of crystal violet dye from aqueous solutions onto date palm fiber by adsorption technique. Journal of Chemistry 2013. doi: 10.1155/2013/210239.

Amarasinghe, B.M.W.P.K. and Williams, R.A. 2007. Tea waste as a low cost adsorbent for the removal of Cu and Pb from wastewater. Chemical Engineering Journal 132(1-3): 299-309. doi: 10.1016/j.cej.2007.01.016.

Barakat, M.A. 2011. New trends in removing heavy metals from industrial wastewater. Arabian journal of chemistry 4(4): 361-377. doi: 10.1016/j.arabjc.2010.07.019.

Calace, N., Di Muro, A., Nardi, E., Petronio, B.M. and Pietroletti, M. 2002. Adsorption isotherms for describing heavy-metal retention in paper mill sludges. Industrial & engineering chemistry research 41(22): 5491-5497. doi: 10.1021/ie011029u.

Calace, N., Nardi, E., Petronio, B.M., Pietroletti, M. and Tosti, G. 2003. Metal ion removal from water by sorption on paper mill sludge. Chemosphere 51(8): 797-803. doi: 10.1016/S0045-6535(02)00864-0.

Chakraborty, S., Chowdhury, S. and Saha, P.D. 2011. Adsorption of crystal violet from aqueous solution onto NaOH-modified rice husk. Carbohydrate Polymers 86(4): 1533-1541. doi: 10.1016/j.carbpol.2011.06.058.

Cheng, H. and Hu, Y. 2010. Lead (Pb) isotopic fingerprinting and its applications in lead pollution studies in China: a review. Environmental pollution 158(5): 1134-1146. doi: 10.1016/j.envpol.2009.12.028.

Cheung, W.H., Szeto, Y.S. and McKay, G. 2007. Intraparticle diffusion processes during acid dye adsorption onto chitosan. Bioresource technology 98(15): 2897-2904. doi: 10.1016/j.biortech.2006.09.045.

Dada, A.O., Olalekan, A.P., Olatunya, A.M. and Dada, O.J.I.J.C. 2012. Langmuir, Freundlich, Temkin and Dubinin–Radushkevich isotherms studies of equilibrium sorption of Zn^{2+} unto phosphoric acid modified rice husk. IOSR Journal of Applied Chemistry 3(1): 38-45. doi: 10.9790/5736-0313845.

Demirbas, A. 2008. Heavy metal adsorption onto agro-based waste materials: a review. Journal of hazardous materials 157(2-3): 220-229. doi: 10.1016/j.jhazmat.2008.01.024.

Devi, P. and Saroha, A.K. 2014. Risk analysis of pyrolyzed biochar made from paper mill effluent treatment plant sludge for bioavailability and eco-toxicity of heavy metals. Bioresource technology 162: 308-315. doi: 10.1016/j.biortech.2014.03.093.

Devi, P. and Saroha, A.K. 2015. Simultaneous adsorption and dechlorination of pentachlorophenol from effluent by Ni–ZVI magnetic biochar composites synthesized from paper mill sludge. Chemical Engineering Journal 271: 195-203. doi: 10.1016/j.cej.2015.02.087.

Devi, P. and Saroha, A.K. 2015. Effect of pyrolysis temperature on polycyclic aromatic hydrocarbons toxicity and sorption behaviour of biochars prepared by pyrolysis of paper mill effluent treatment plant sludge. Bioresource technology 192: 312-320. doi: 10.1016/j.biotech.2015.05.084.

Elmorsi, T.M., Mohamed, Z.H., Shopak, W. and Ismaiel, A.M. 2014. Kinetic and equilibrium isotherms studies of adsorption of Pb (II) from water onto natural adsorbent. Journal of Environmental Protection 5(17): 1667. doi: 10.4236/jep.2014.517157.

Febrianto, J., Kosasih, A.N., Sunarso, J., Ju, Y.H., Indraswati, N. and Ismadji, S. 2009. Equilibrium and kinetic studies in adsorption of heavy metals using biosorbent: a summary of recent studies. Journal of hazardous materials 162(2-3): 616-645. doi: 10.1016/j.jhazmat.2008.06.042.

Feng, L.F. and Qi, W. 2011. Removal of heavy metal ions from wastewaters. Journal of Environmental Management 92(3): 407-418. doi: 10.1016/j.jenvman.2010.11.011.

Foo, K.Y. and Hameed, B.H. 2010. Insights into the modeling of adsorption isotherm systems. Chemical engineering journal 156(1): 2-10. doi: 10.1016/j.cej.2009.09.013.

Forgacs, E., Cserhati, T. and Oros, G. 2004. Removal of synthetic dyes from wastewaters: a review. Environment international 30(7): 953-971. doi: 10.1016/j.envint.2004.02.001.

Gidlow, D.A. 2004. Lead toxicity. Occupational medicine 54(2): 76-81. doi: 10.1093/occmed/kqh019.

Gorzin, F. and Bahri Rasht Abadi, M.M. 2018. Adsorption of Cr (VI) from aqueous solution by adsorbent prepared from paper mill sludge: Kinetics and thermodynamics studies. Adsorption Science & Technology 36(1-2): 149-169. doi: 10.1177/0263617416686976.

Gregory, P. 1990. Classification of dyes by chemical structure. In The Chemistry and Application of Dyes, p. 17-47. Springer, Boston, MA. doi: 10.1007/978-1-4684-7715-3_2.

Gupta, V.K., Agarwal, S. and Saleh, T.A. 2011. Synthesis and characterization of alumina-coated carbon nanotubes and their application for lead removal. Journal of hazardous materials 185(1): 17-23. doi: 10.1016/j.jhazmat.2010.08.053.

Hall, K.R., Eagleton, L.C., Acrivos, A. and Vermeulen, T. 1966. Pore-and solid-diffusion kinetics in fixed-bed adsorption under constant-pattern conditions. Industrial & engineering chemistry fundamentals 5(2): 212-223.

Hameed, B.H., Ahmad, A.A. and Aziz, N. 2007. Isotherms, kinetics and thermodynamics of acid dye adsorption on activated palm ash. Chemical Engineering Journal 133(1-3): 195-203. doi: 10.1016/j.cej.2007.01.032.

Ho, Y.S. and McKay, G. 1999. Pseudo-second order model for sorption processes. Process biochemistry 34(5): 451-465.

Hunger, K. ed. 2007. Industrial dyes: chemistry, properties, applications. John Wiley & Sons. doi: 10.1002/3527602011.

Inyang, M. and Dickenson, E. 2015. The potential role of biochar in the removal of organic and microbial contaminants from potable and reuse water: a review. Chemosphere 134: 232-240. doi: 10.1016/j.chemosphere.2015.03.072.

Inyang, M., Gao, B., Yao, Y., Xue, Y., Zimmerman, A.R., Pullammanappallil, P. and Cao, X. 2012. Removal of heavy metals from aqueous solution by biochars derived from anaerobically digested biomass. Bioresource technology 110: 50-56. doi: 10.1016/j.biortech.2012.01.072.

Inyang, M.I., Gao, B., Yao, Y., Xue, Y., Zimmerman, A., Mosa, A., Pullammanappallil, P., Ok, Y.S. and Cao, X. 2016. A review of biochar as a low-cost adsorbent for aqueous heavy metal removal. Critical Reviews in Environmental Science and Technology 46(4): 406-433. doi: 10.1080/10643389.2015.1096880.

Jaishankar, M., Tseten, T., Anbalagan, N., Mathew, B.B. and Beeregowda, K.N. 2104. Toxicity, mechanism and health effects of some heavy metals. Interdisciplinary toxicology 7(2): 60-72. doi: 10.2478/intox-2014-0009.

Jaman, H., Chakraborty, D. and Saha, P. 2009. A study of the thermodynamics and kinetics of copper adsorption using chemically modified rice husk. CLEAN–Soil, Air, Water 37(9): 704-711. doi: 10.1002/clen.200900138.

Jung, K.W., Hwang, M.J., Ahn, K.H. and Ok, Y.S. 2015. Kinetic study on phosphate removal from aqueous solution by biochar derived from peanut shell as renewable adsorptive media. International journal of environmental science and technology 12(10): 3363-3372. doi: 10.1007/s13762-015-0766-5.

Kalavathy, M.H., Karthikeyan, T., Rajgopal, S. and Miranda, L.R. 2005. Kinetic and isotherm studies of Cu (II) adsorption onto H_3PO_4-activated rubber wood sawdust. Journal of colloid and interface science 292(2): 354-362. doi: 10.1016/j.jcis.2005.05.087.

Králik, M. 2014. Adsorption, chemisorption, and catalysis. Chemical Papers 68(12): 1625-1638. doi: 10.2478/s11696-014-0624-9.

Lagergren, S.K. 1898. About the theory of so-called adsorption of soluble substances. Sven. Vetenskapsakad. Handingarl 24: 1-39.

Lin, L., Jiang, W. and Xu, P. 2017. Comparative study on pharmaceuticals adsorption in reclaimed water desalination concentrate using biochar: Impact of salts and organic matter. Science of the Total Environment 601: 857-864. doi: 10.1016/j.scitotenv.2017.05.203.

Lister, S.K. and Line, M.A. 2001. Potential utilisation of sewage sludge and paper mill waste for biosorption of metals from polluted waterways. Bioresource Technology 79(1): 35-39. doi: 10.1016/S0960-8524(01)00035-9.

Lonappan, L., Rouissi, T., Brar, S.K., Verma, M. and Surampalli, R.Y. 2018. An insight into the adsorption of diclofenac on different biochars: Mechanisms, surface chemistry, and thermodynamics. Bioresource technology 249: 386-394.

Malkoc, E. and Nuhoglu, Y. 2005. Investigations of nickel (II) removal from aqueous solutions using tea factory waste. Journal of hazardous materials 127(1-3): 120-128. doi: 10.1016/j.jhazmat.2005.06.030.

Mall, I.D., Srivastava, V.C. and Agarwal, N.K. 2006. Removal of Orange-G and Methyl Violet dyes by adsorption onto bagasse fly ash - kinetic study and equilibrium isotherm analyses. Dyes and pigments 69(3): 210-223. doi: 10.1016/j.dyepig.2005.03.013.

Méndez, A., Barriga, S., Fidalgo, J.M. and Gascó, G. 2009. Adsorbent materials from paper industry waste materials and their use in Cu (II) removal from water. Journal of Hazardous Materials 165(1-3): 736-743. doi: 10.1016/j.jhazmat.2008.10.055.

Mittal, A., Mittal, J., Malviya, A., Kaur, D. and Gupta, V.K. 2010. Adsorption of hazardous dye crystal violet from wastewater by waste materials. Journal of colloid and interface science 343(2): 463-473. doi: 10.1016/j.jcis.2009.11.060.

Mohan, D., Sarswat, A., Ok, Y.S. and Pittman Jr, C.U. 2014. Organic and inorganic contaminants removal from water with biochar, a renewable, low cost and sustainable adsorbent–a critical review. Bioresource technology 160: 191-202. doi: 10.1016/j.biortech.2014.01.120.

Nandal, M., Hooda, R. and Dhania, G. 2014. Tea wastes as a sorbent for removal of heavy metals from wastewater. International Journal of Current Engineering and Technology 4(1): 1-5.

Nargawe, T., Rai, A.K., Ameta, R. and Ameta, S.C. 2018. Adsorption study for removal of crystal violet dye using MMT-MWCNTs composite from aqueous solution, Journal of Applicable Chemistry 7(5): 1252-1259.

Ngah, W.W. and Hanafiah, M.M. 2008. Removal of heavy metal ions from wastewater by chemically modified plant wastes as adsorbents: a review. Bioresource technology 99(10): 3935-3948. http://dx.doi.org/10.1016/j.spc.

Oliveira, F.R., Patel, A.K., Jaisi, D.P., Adhikari, S., Lu, H. and Khanal, S.K. 2017. Environmental application of biochar: Current status and perspectives. Bioresource technology 246: 110-122. doi: 10.1016/j.biortech.2017.08.122.

Perić, J., Trgo, M. and Medvidović, N.V. 2004. Removal of zinc, copper and lead by natural zeolite—a comparison of adsorption isotherms. Water research 38(7): 1893-1899. doi: 10.1016/j.watres.2003.12.035.

Qi, B.C. and Aldrich, C. 2008. Biosorption of heavy metals from aqueous solutions with tobacco dust. Bioresource Technology 99(13): 5595-5601. doi: 10.1016/j.biortech.2007.10.042.

Qiu, H., Lv, L., Pan, B.C., Zhang, Q.J., Zhang, W.M. and Zhang, Q.X. 2009. Critical review in adsorption kinetic models. Journal of Zhejiang University-Science A 10(5): 716-724. doi: 10.1631/jzus.A0820524.

Renberg, I., Brännvall, M.L., Bindler, R. and Emteryd, O. 2002. Stable lead isotopes and lake sediments—a useful combination for the study of atmospheric lead pollution history. Science of the Total Environment 292(1-2): 45-54. doi: 10.1016/S0048-9697(02)00032-3.

Schwarzenbach, R.P., Egli, T., Hofstetter, T.B., Von Gunten, U. and Wehrli, B. 2010. Global water pollution and human health. Annual review of environment and resources 35: 109-136. doi: 10.1146/annurev-environ-100809-125342.

Seker, S. 2014. Determination of copper (Cu) levels for rivers in Tunceli, Turkey. doi: 10.5923/j.env.20140404.02.

Sewu, D.D., Boakye, P., Jung, H. and Woo, S.H. 2017. Synergistic dye adsorption by biochar from co-pyrolysis of spent mushroom substrate and Saccharina japonica. Bioresource technology 244: 1142-1149. doi: 10.1016/j.biortech.2017.08.103.

Sewu, D.D., Boakye, P. and Woo, S.H. 2017. Highly efficient adsorption of cationic dye by biochar produced with Korean cabbage waste. Bioresource technology 224: 206-213. doi: 10.1016/j.biortech.2016.11.009.

Suryan, S. and Ahluwalia, S.S. 2012. Biosorption of heavy metals by paper mill waste from aqueous solution. International Journal of Environmental Sciences 2(3): 1331-1343. doi: 10.6088/ijes.00202030020.

Tan, X.F., Liu, Y.G., Gu, Y.L., Liu, S.B., Zeng, G.M., Cai, X., Hu, X.J., Wang, H., Liu, S.M. and Jiang, L.H. 2016. Biochar pyrolyzed from MgAl-layered double hydroxides pre-coated ramie biomass (Boehmeria nivea (L.) Gaud.): characterization and application for crystal violet removal. Journal of environmental management 184: 85-93. doi: 10.1016/j.jenvman.2016.08.070.

Tchounwou, P.B., Yedjou, C.G., Patlolla, A.K., Sutton, D.J. and Luch, A. 2012. Molecular, clinical and environmental toxicology. Molecular, Clinical and Environmental Toxicology 3: 133-164. doi: 10.1007/978-3-7643-8340-4.

Thakur, L.S. and Parmar, M. 2013. Adsorption of heavy metal (Cu^{2+}, Ni^{2+} and Zn^{2+}) from synthetic waste water by tea waste adsorbent. International Journal of Chemical and Physical Sciences 2(6): 6-19. Available at: http://www.ijcps.org/admin/php/uploads/52_pdf.pdf.

Thommes, M., Kaneko, K., Neimark, A.V., Olivier, J.P., Rodriguez-Reinoso, F., Rouquerol, J. and Sing, K.S. 2015. Physisorption of gases, with special reference to the evaluation of surface area and pore size distribution (IUPAC Technical Report). Pure and Applied Chemistry 87(9-10): 1051-1069. doi: 10.1515/pac-2014-1117.

Titi, O.A. and Bello, O.S. 2015. An overview of low cost adsorbents for copper (II) ions removal. Journal of Biotechnology & Biomaterials 5(1): 1. doi: 10.4172/2155-952X.1000177.

Varma, G., Singh, R.K. and Sahu, V. 2013. A comparative study on the removal of heavy metals by adsorption using fly ash and sludge: a review. International Journal of Application or Innovation in Engineering and Management 2(7): 45-56.

Vyavahare, G., Jadhav, P., Jadhav, J., Patil, R., Aware, C., Patil, D., Gophane, A., Yang, Y.H. and Gurav, R. 2019. Strategies for crystal violet dye sorption on biochar derived from mango leaves and evaluation of residual dye toxicity. Journal of Cleaner Production 207: 296-305. doi: 10.1016/j.jclepro.2018.09.193.

Wajima, T. 2014. Preparation of adsorbent with lead removal ability from paper sludge using sulfur-impregnation. APCBEE procedia 10(10): 164-169. doi: 10.1016/j.apcbee.2014.10.001.

Wasewar, K.L. 2010. Adsorption of metals onto tea factory waste: a review. International Journal of Research and Reviews in Applied Sciences 3(3): 303. Available at: http://www.arpapress.com/Volumes/Vol3Issue3/IJRRAS_3_3_09.pdf.

Wathukarage, A., Herath, I., Iqbal, M.C.M. and Vithanage, M. 2019. Mechanistic understanding of crystal violet dye sorption by woody biochar: implications for wastewater treatment. Environmental geochemistry and health 41(4): 1647-1661. doi: 10.1007/s10653-017-0013-8.

Wong, Y. and Yu, J. 1999. Laccase-catalyzed decolorization of synthetic dyes. Water research 33(16): 3512-3520.

Yi, S., Gao, B., Sun, Y., Wu, J., Shi, X., Wu, B. and Hu, X. 2016. Removal of levofloxacin from aqueous solution using rice-husk and wood-chip biochars. Chemosphere 150: 694-701. doi: 10.1016/j.chemosphere.2015.12.112.

Yoon, K., Cho, D.W., Tsang, D.C., Bolan, N., Rinklebe, J. and Song, H. 2017. Fabrication of engineered biochar from paper mill sludge and its application into removal of arsenic and cadmium in acidic water. Bioresource technology 246: 69-75. doi: 10.1016/j.biortech.2017.07.020.

Zou, W., Han, R., Chen, Z., Jinghua, Z. and Shi, J. 2006. Kinetic study of adsorption of Cu (II) and Pb (II) from aqueous solutions using manganese oxide coated zeolite in batch mode. Colloids and Surfaces A: Physicochemical and Engineering Aspects 279(1-3): 238-246. doi: 10.1016/j.colsurfa.2006.01.008.